Palaeogeography, Palaeoclimatology, Palaeoecology 302 (2011) 435–451

Contents lists available at ScienceDirect

Palaeogeography, Palaeoclimatology, Palaeoecology

journal homepage: www.elsevier.com/locate/palaeo

Blake Outer Ridge: Late Neogene variability in paleoceanography and deep-sea biota

Ajoy K. Bhaumik [a,*], Anil K. Gupta [b,1], Ellen Thomas [c,d,2]

[a] Department of Applied Geology, Indian School of Mines, Dhanbad 826 004, India
[b] Department of Geology and Geophysics, Indian Institute of Technology, Kharagpur 721 302, India
[c] Department of Geology and Geophysics, Yale University, P.O. Box 208109, New Haven, CT 06520-8109, USA
[d] Department of Earth and Environmental Sciences, Wesleyan University, Middletown, CT 06459-0139, USA

ARTICLE INFO

Article history:
Received 16 November 2010
Received in revised form 2 February 2011
Accepted 6 February 2011
Available online 15 February 2011

Keywords:
Benthic foraminifera
Stable isotopes
Total Organic Carbon
Northern Hemisphere Glaciation
Southern Component Water
Northern Component Water

ABSTRACT

Carbon isotope and benthic foraminiferal data from Blake Outer Ridge, a sediment drift in the western North Atlantic (Ocean Drilling Program Sites 994 and 997, water depth ~2800 m), document variability in the relative volume of Southern Component (SCW) and Northern Component Waters (NCW) over the last 7 Ma. SCW was dominant before ~5.0 Ma, at ~3.6–2.4 Ma, and 1.2–0.8 Ma, whereas NCW dominated in the warm early Pliocene (5.0–3.6 Ma), and at 2.4–1.2 Ma. The relative volume of NCW and SCW fluctuated strongly over the last 0.8 Ma, with strong glacial–interglacial variability. The intensity of the Western Boundary Undercurrent was positively correlated to the relative volume of NCW. Values of Total Organic Carbon (TOC) were >1.5% in sediments older than ~3.8 Ma, and not correlated to high primary productivity indicators, thus may reflect lateral transport of organic matter. TOC values decreased during the intensification of the Northern Hemisphere Glaciation (NHG, 3.8–1.8 Ma). Benthic foraminiferal assemblages underwent major changes when the sites were dominantly under SCW (3.6–2.4 and 1.2–0.8 Ma), coeval with the 'Last Global Extinction' of elongate, cylindrical deep-sea benthic foraminifera, which has been linked to cooling, increased ventilation and changes in the efficiency of the biological pump. These benthic foraminiferal turnovers were neither directly associated with changes in dominant bottom water mass nor with changes in productivity, but occurred during global cooling and increased ventilation of deep waters associated with the intensification of the NHG.

1. Introduction

Blake Outer Ridge (BOR) in the westernmost part of the North Atlantic Ocean (Fig. 1) is a sediment drift, adjacent to two important components of the Atlantic Meridional Overturning Circulation: the warm, saline Gulf Stream and the deep Western Boundary Undercurrent (WBUC). The BOR, built-up of fine grained nannofossil-bearing hemipelagic sediments (Paull et al., 1996), has been argued to have formed through interaction between the upper part of the WBUC and the lower part of the Gulf Stream, where it detaches from the continental slope (e.g., Stahr and Sanford, 1999). BOR sediments largely consist of material transported from the Canadian continental margin by the WBUC (Reynolds et al., 1999; Balsam and Damuth, 2000) (Fig. 1).

Presently, the flanks of the BOR above ~3500 m are covered by the Northern Component Waters (NCW), carried by the WBUC to the South, with a density of ~27.88 kg/m^3 and a dissolved oxygen concentration of ~6.3 ml/L (Bower and Hunt, 2000). The NCW consists of several water masses, including the Upper North Atlantic Deep Water (UNADW) with Labrador Sea Waters at depths shallower than ~2500 m, and Lower North Atlantic Deep Water (LNADW, or Norwegian–Greenland Sea Overflow Water), between ~2500 and 4000 m (Stahr and Sanford, 1999; Evans and Hall, 2008). At depths greater than ~4000 m, the BOR is covered by Southern Component Waters (SCW), mainly fed by the Antarctic Bottom Water (AABW). This bottom watermass, however, consists of a varying mixture of NCW (up to 90%) and SCW (Stahr and Sanford, 1999), where the southern component has been recirculated in a cyclonic gyre north of the BOR, and therefore has the same flow direction as the overlying LNADW at the BOR (Weatherly and Kelley, 1985).

The BOR is thus an important region in the North Atlantic Meridional Overturning Circulation (MOC), and vital for the latitudinal exchange of heat, salt and water (Raymo et al., 1990; Evans and Hall, 2008). The BOR underlies the periphery of the subtropical central gyre, with weak upwelling supplying nutrients to the phytoplankton. Over time, the margin of the gyre has migrated repeatedly, so that the

* Corresponding author. Tel.: +91 326 223 5684; fax: +91 326 229 6616.
E-mail addresses: ajoyism@gmail.com (A.K. Bhaumik), anilg@gg.iitkgp.ernet.in (A.K. Gupta), ellen.thomas@yale.edu, ethomas@wesleyan.edu (E. Thomas).
[1] Tel.: +91 3222 283368; fax: +91 3222 255303.
[2] Tel.: +1 2032 432 5928, +1 860 685 2238; fax: +1 203 432 3134, +1 860 685 3651.

0031-0182/$ – see front matter © 2011 Elsevier B.V. All rights reserved.
doi:10.1016/j.palaeo.2011.02.004

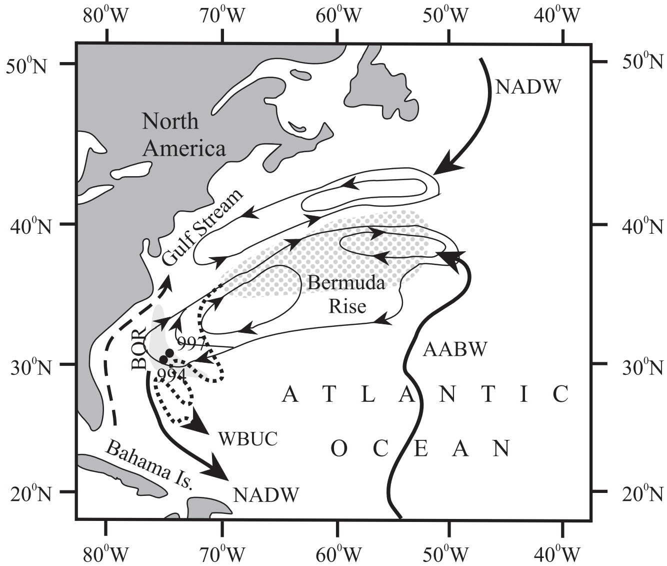

Fig. 1. Location map of ODP Holes 994C and 997A within the oceanographic setting of the Blake Outer Ridge area. Thick solid and dotted lines indicate deep ocean currents and segmented line indicates surface ocean currents at Blake Outer Ridge (BOR) area, Northwest Atlantic. Thin lines with arrows represent subtropical gyres. Figure is redrawn from report of Shipboard Scientific Party (1998). NADW, AABW and WBUC represent North Atlantic Deep Water, Antarctic Bottom Water and Western Boundary Undercurrent, respectively.

more oligotrophic central gyre regions were over the BOR for some periods of time (e.g., Ikeda et al., 2000; Okada, 2000).

BOR sediments have been studied extensively to understand paleoceanographic changes during the Pleistocene and Holocene (Amos et al., 1971; Haskell et al., 1991; Luo et al., 2001; Franz and Tiedemann, 2002; Giosan et al., 2002; Thunell et al., 2002; Roth and Reijmer, 2004; Gutjahr et al., 2008). Proxies include sediment grain size (Haskell et al., 1991; Evans and Hall, 2008), sediment chemistry (Giosan et al., 2002), Al–Be–Th isotopic ratios of sediments (Luo et al., 2001), Nd isotopes (Gutjahr et al., 2008), and foraminiferal carbon and oxygen isotope ratios (Franz and Tiedemann, 2002; Thunell et al., 2002; Roth and Reijmer, 2004). These studies document that the depth of the contact between NCW (above) and SCW (below) has changed significantly over time, generally shallowing by more than 2000 m during glacial intervals, so that the WBUC's zone of maximum flow speed shifted to a depth of less than 2500 m (Evans and Hall, 2008). The glacial counterpart of the North Atlantic Deep Water (NADW), commonly called the Glacial North Atlantic Intermediate Water (GNAIW) (Marchitto et al., 1998; Franz and Tiedemann, 2002) thus remained at much shallower depths than the present-day NADW, and may have sunk from the surface considerably further to the South (Lynch-Stieglitz et al., 2007; Evans and Hall, 2008).

There have been fewer studies to reconstruct the relative volume of NCW and SCW during earlier time periods. Reynolds et al. (1999) and Frank et al. (2002) used Nd and Pb isotope studies to argue that the export of the SCW was strong prior to 3 Ma, and linked changes in Pb isotope values after 3 Ma and more dramatic changes since 1.8 Ma to the north Atlantic circulation as related to the Northern Hemisphere Glaciation (NHG). Poore et al. (2006) used compilations of high-resolution benthic stable isotope data to reconstruct the percent NCW over the last 12 Ma, linking periods of high NCW volume (thus a large volume of Norwegian–Greenland Sea Overflow Water), to times of tectonic lowering of the Greenland–Scotland Ridge, with highest volumes of NCW between 5.5 and 2.5 Ma.

This study uses benthic foraminiferal census and isotope data combined with Total Organic Carbon (TOC) data from Ocean Drilling Program (ODP) Holes 994C and 997A to reconstruct the late Neogene paleoceanographic and paleoenvironmental evolution of the BOR. Benthic foraminifera are an important proxy to reconstruct paleoceanographic changes in the deep-sea, reflecting the availability and quality of particulate organic carbon (food particles, specifically labile as compared to refractory components), the seasonality or lack thereof of the food supply, and bottom/pore water oxygen concentration, although factors such as bottom current intensity may also play a role (Sen Gupta and Machain-Castillo, 1993; Loubere and Fariduddin, 1999; Gooday, 2003; Fontanier et al., 2005; Jorissen et al., 2007). We selected high sedimentation rate (Paull et al., 1996) ODP Holes 994C and 997A on the Blake Ridge to increase our understanding of late Neogene deep-sea paleoceanographic changes. We generated a 7 myr record of benthic foraminiferal census data from Holes 994C and 997A, stable carbon and oxygen data on tests of *Cibicides* species and *Oridorsalis umbonatus*, and data on the organic carbon content of the bulk sediment from Hole 994C. We compared our data with published records of local primary productivity based on diatoms [Site 997, (Ikeda et al., 2000)], calcareous nannoplankton [Site 994C, (Okada, 2000)], and oxygen and carbon isotopic records of diagenetic carbonate from Hole 994C (Pierre et al., 2000).

2. Materials and methods

ODP Holes 994C (31° 47.139′ N; 75° 32.753′ W; present day water depth 2799.1 m; penetration 703.5 meters below sea floor or mbsf) and 997A (31° 50.588′ N; 75° 28.118′ W; present day water depth 2770.1 m; penetration 434.3 mbsf) were drilled during ODP Leg 164, and are located 9.6 km apart on the crest of the BOR [(Paull et al., 1996), Fig. 1]. The sediment accumulation rate of the hemipelagic oozes was high during the late Miocene (average ~11 cm/kyr at 994C and ~8 cm/kyr at 997A) and Pliocene (~12.5 cm/kyr at 994C; ~10 cm/kyr at 997A), but during the Pleistocene dropped to ~5.5 cm/kyr at 994C and ~4.6 cm/kyr at 997A (Fig. 2). Disseminated gas hydrate occurs throughout the sedimentary section between ~450 and ~180 mbsf (~5 to ~2.9 Ma) in both holes (Paull et al., 1996). Free gaseous methane is present below 450 mbsf, but sediments above 180 mbsf (<2.9 Ma) are devoid of gas hydrate. On BOR, cold methane seeps have been found at ~2150 m water depth (Van Dover et al., 2003; Robinson et al., 2004). There is, however, no evidence that methane from the gas hydrates reached the sea floor in cold seeps at the location of Sites 994 and 997, thus benthic foraminiferal assemblages probably were not exposed to methane seeps (Paull et al., 1996). The source organic matter of the clathrate methane may date to the Paleogene, much older than the sediments in which the hydrates reside (Fehn et al., 2000).

2.1. Faunal analysis

We analyzed 440 (Hole 994C) and 240 (Hole 997A) sediment samples of 10 cm^3 volume. Samples were processed following Gupta and Thomas (1999). Samples were soaked in water with baking soda for 8–10 h. A few drops of hydrogen peroxide (2%) were added to indurated samples in order to improve disaggregation. Wet samples were washed over a 63 μm size sieve, then dry-sieved over a 125 μm sieve. The >125 μm size fraction was used for microscopic examination and census counts of benthic foraminifera. Processed samples were split into suitable aliquots to obtain about 250–300 specimens of benthic foraminifera per sample. A total of 220 and 160 species were recorded from Holes 994C and 997A, respectively, among which 137 species are common in both holes. Of these, 48 species contribute significantly to the total population (combined from both holes), occurring in more than 100 samples with at least 8% relative abundance in at least one sample. Eighty three species from Hole 994C and 23 species from Hole 997A occur as rare species only, i.e. present in one to five samples at less than 5% relative abundance. Specimens from both sites are generally well preserved, are not

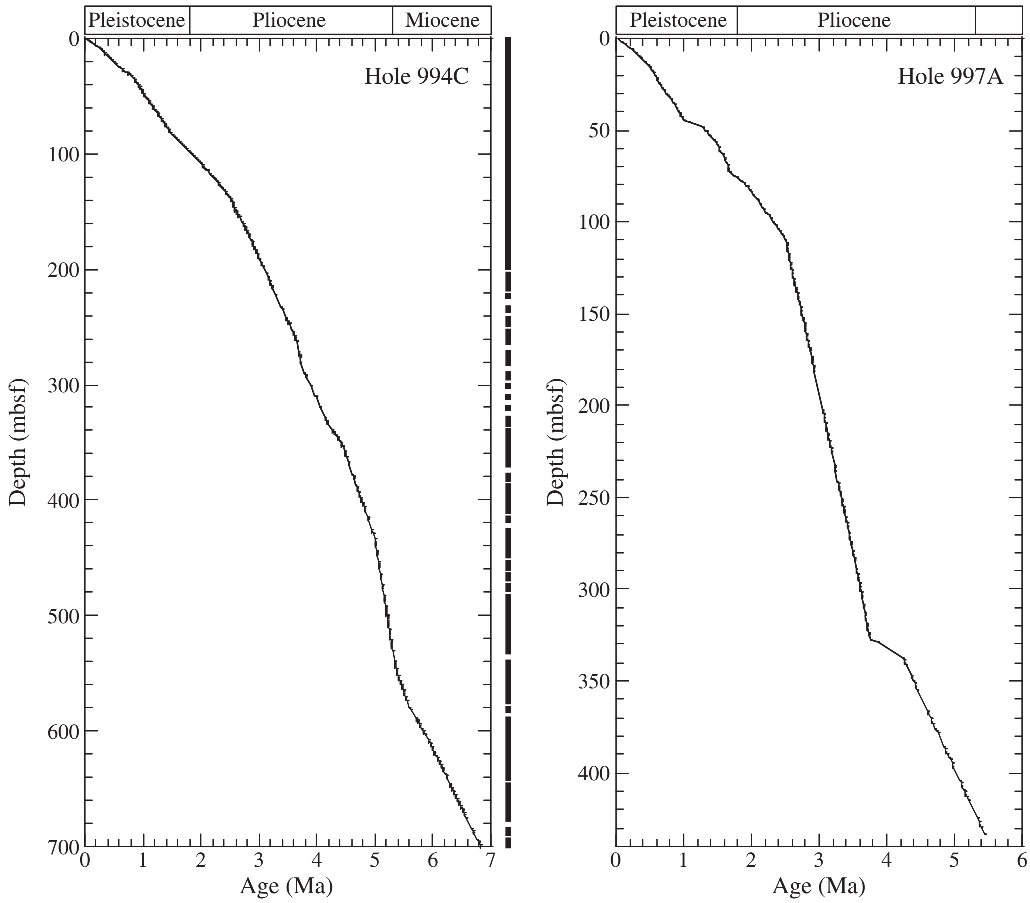

Fig. 2. Depth versus age plots of Holes 994C and 997A based on nannofossil data (Okada, 2000). Distribution of samples through depths at Holes 994C and 997A is given in the right side of each graph.

yellowed or highly polished or badly abraded, thus do not show clear signs of reworking. The average age interval is ~15.4 kyr per sample at Hole 994C and ~22.1 kyr at Hole 997A. Separate age models for both sites (Fig. 2) are based on biostratigraphic data (Okada, 2000), as correlated to the numerical time scale of Berggren et al. (1995). Our time resolution cannot resolve precessional and obliquity-paced variability, and our main purpose was to document the longer-time scale paleoceanographic changes.

2.2. Multivariate analysis

Holes 994C and 997A are located close to each other both geographically and bathymetrically, and common species occur at both holes. Therefore, we combined the faunal data from both holes in the statistical analysis. We selected 48 common species with a relative abundance of 8% or more in at least one sample and present in at least 100 samples for factor and cluster analyses using the SAS/STAT package (Appendix 1).

R-mode Principal Component Analysis (PCA) was performed on the correlation matrix followed by an orthogonal VARIMAX rotation to maximize the variance. Based on the scree (x–y) plot of eigen values versus the number of species (variables) and screening of factor scores we retained 9 factors (Table 1, Fig. 3) that account for 47.9% of the total variance. This low variance may be related to the large number of variables (i.e., species) over the studied interval and the large number of samples (680). We used zero to designate the missing values of each species against each observation number in PCA analysis.

We performed Q-mode cluster analysis using Ward's Minimum Variance method. Prior to cluster analysis, a PCA was performed on the covariance matrix of the 48 highest ranked species from both holes to standardize the dataset. Based on the plot of semi-partial R-squared values versus the number of clusters, nine clusters were identified (Appendix 2). VARIMAX-rotated factors that show high factor scores with well-established species associations were used to identify biofacies. We identified 9 biofacies, and interpreted their paleoenvironments based on present day ecological preferences of the most abundant species in the biofacies (Tables 1 and 2).

2.3. Total Organic Carbon analysis

Total Organic Carbon (TOC) analysis was performed on 0.5 g of finely powdered, oven-dried sediment, which was dissolved in 50 ml water with 20 drops of 1 N HCl solution. Samples were placed for two hours at room temperature on a magnetic stirrer to digest inorganic carbon. Solutions were analyzed using a TOC Analyzer (TOC-V_{CPH}; Shimadzu Corporation, Japan) in the TOC-GC laboratory, Department of Geology and Geophysics, Indian Institute of Technology, Kharagpur. 2 N HCl and 25% phosphoric acid was further added and purged for 1.5 min for complete digestion of inorganic carbon, and to bring the pH of the solution to 2–3. The machine was standardized using a KH Phthalate synthetic standard. The calibration curve was drawn through the scatter readings of 8 standard solutions (10, 25, 50, 100, 200, 300, 400, and 500 ppm). For the analysis of each sample, 2 to 5 injections were chosen, taking the average of two readings with a standard deviation less than 0.1 and a coefficient of variance less than

Table 1
Benthic foraminiferal biofacies with their factor scores and preferred environments at Hole 994C and 997A.

Biofacies	% variance	Factor scores	Environment
Uhc–Uh (factor 1 + ve)			
Uvigerina hispida	6.15542	0.76913	High organic carbon, independent of bottom water oxygenation
Uvigerina hispido-costata		0.72611	
Uvigerina peregrina		0.27672	
Globocassidulina tumida		0.22165	
Ou–Pb (factor 3 + ve)			
Oridorsalis umbonatus	5.624418	−0.51477	Cosmopolitan, well oxygenated, relatively low organic carbon
Pullenia bulloides		−0.21869	
Bp–Bp (factor 5 + ve)			
Bolivina pseudopunctata	5.36591	0.70542	High organic carbon, possibly low oxygen; *S. lepidula* belongs to the 'extinction group' taxa; miliolids generally indicate well oxygenated environment, however
Bolivina paula		0.48213	
Fursenkoina fusiformis		0.36347	
Cibicides bradyi		0.26770	
Pyrgo lucernula		0.25376	
Stilostomella lepidula		0.25016	
Nonionella auris		0.24580	
Gc–Pb (factor 7 + ve)			
Gyroidinoides cibaoensis	5.31194	0.69072	Intermediate to high organic carbon flux and low oxygen, possibly influence of bottom currents
Pullenia bulloides		0.37708	
Cibicides bradyi		0.32291	
Gyroidinoides nitidula		0.26764	
Sphaeroidina bulloides		0.25427	
Quinqueloculina weaveri		0.25034	
Globocassidulina subglobosa		0.22933	
Sc–Pa (factor 8 + ve)			
Stilostomella consobrina	5.11329	0.70536	All taxa in this group are 'extinction group', seen as indicative of overall medium-high food supply, probably well oxygenated
Pleurostomella alternans		0.38673	
Nodosaria longiscata		0.34619	
Dentalina stimulea		0.26418	
Fa–Rg (factor 10 + ve)			
Frondicularia advena	5.01030	0.73723	Low to intermediate organic carbon
Robulus gibbus		0.49046	
Glandulina laevigata		0.26040	
Sl–Mp(factor 4 − ve)			
Stilostomella lepidula	5.45012	−0.52603	Intermediate organic flux, possibly refractory organic carbon (*Stilostomella lepidula* and *Pleurostomella alternans* are extinction group of species)
Melonis pompilioides		−0.29202	
Astrononian umbilicatulum		−0.22263	
Pleurostomella alternans		−0.20075	
Gp–Au (factor 12 + ve)			
Globobulimina pacifica	4.90002	0.76180	High organic carbon, potentially low oxygen; refractory organic carbon
Astrononian umbilicatulum		0.34979	
Pullenia quinqueloba		0.24438	
Cc–Ba(factor 11 + ve)			
Cassidulina carinata	4.99278	0.77873	Intermediate organic carbon flux, possibly with high seasonality
Bulimina alazanensis		0.53090	

2% as the final value. TOC analysis were performed on 447 samples from Hole 994C.

2.4. Stable isotope analysis

Five to ten individuals of *Oridorsalis umbonatus*, a common species present in most samples, were picked from 191 samples from Hole 994C for stable carbon and oxygen isotope analysis. In samples where *O. umbonatus* specimens were rare, *Cibicides wuellerstorfi*, *Cibicides kullenbergi* and/or *Cibicides bradyi* were analyzed. Pre-cleaned samples were reacted in 100% orthophosphoric acid at 70 °C using a Finnigan-MAT Kiel III carbonate preparation device. Evolved CO_2 gas was measured online with the Finnigan-MAT 252 Mass Spectrometer at the University of Florida, with standard NBS-19 for calibration. Isotopic results are reported in standard delta notation relative to Vienna Pee Dee Belemnite (VPDB). Analytical precision is estimated (1 standard deviation of standards run with samples) to be ±0.02‰ for $\delta^{13}C$ and ±0.07‰ for $\delta^{18}O$ (n = 58). To correct for the isotopic offset of oxygen and carbon isotope values (vital/habitat effect) between the shallow infaunal *O. umbonatus* and the epifaunal *C. wuellerstorfi*, stable isotope values were adjusted to *C. wuellerstorfi* using the scale "$\delta^{13}C$ of *C. wuellerstorfi* = $\delta^{13}C$ of *O. umbonatus* + 1‰" and "$\delta^{18}O$ of *C. wuellerstorfi* = $\delta^{18}O$ of *O. umbonatus* − 0.5‰" (Shackleton et al., 1984). The $\delta^{18}O$ values of *C. wuellerstorfi* were adjusted to equilibrium with sea water by adding 0.64‰ (Shackleton et al., 1984; Zachos et al., 2001).

2.5. SEM study

Diagenetic carbonate nodules are common in both holes (Pierre et al., 2000). The formation of diagenetic calcite may be responsible for changes in oxygen and carbon isotopic values because the foraminiferal tests may contain post-depositional, authigenic carbonates. In gas hydrate containing sediments as recovered at Sites 994 and 997, authigenic calcite may have highly depleted $\delta^{13}C$ values [around −20‰, (e.g., Millo et al., 2005)]. To examine whether benthic foraminifera have undergone diagenetic changes, SEM photographs of broken specimens of a few species from Hole 994C were taken from 10 randomly picked samples (Fig. 4, Table 3).

3. Results

3.1. Biofacies distribution

Multivariate analysis of faunal data helps to remove noise from the data set induced by post-mortem taphonomic processes and make it

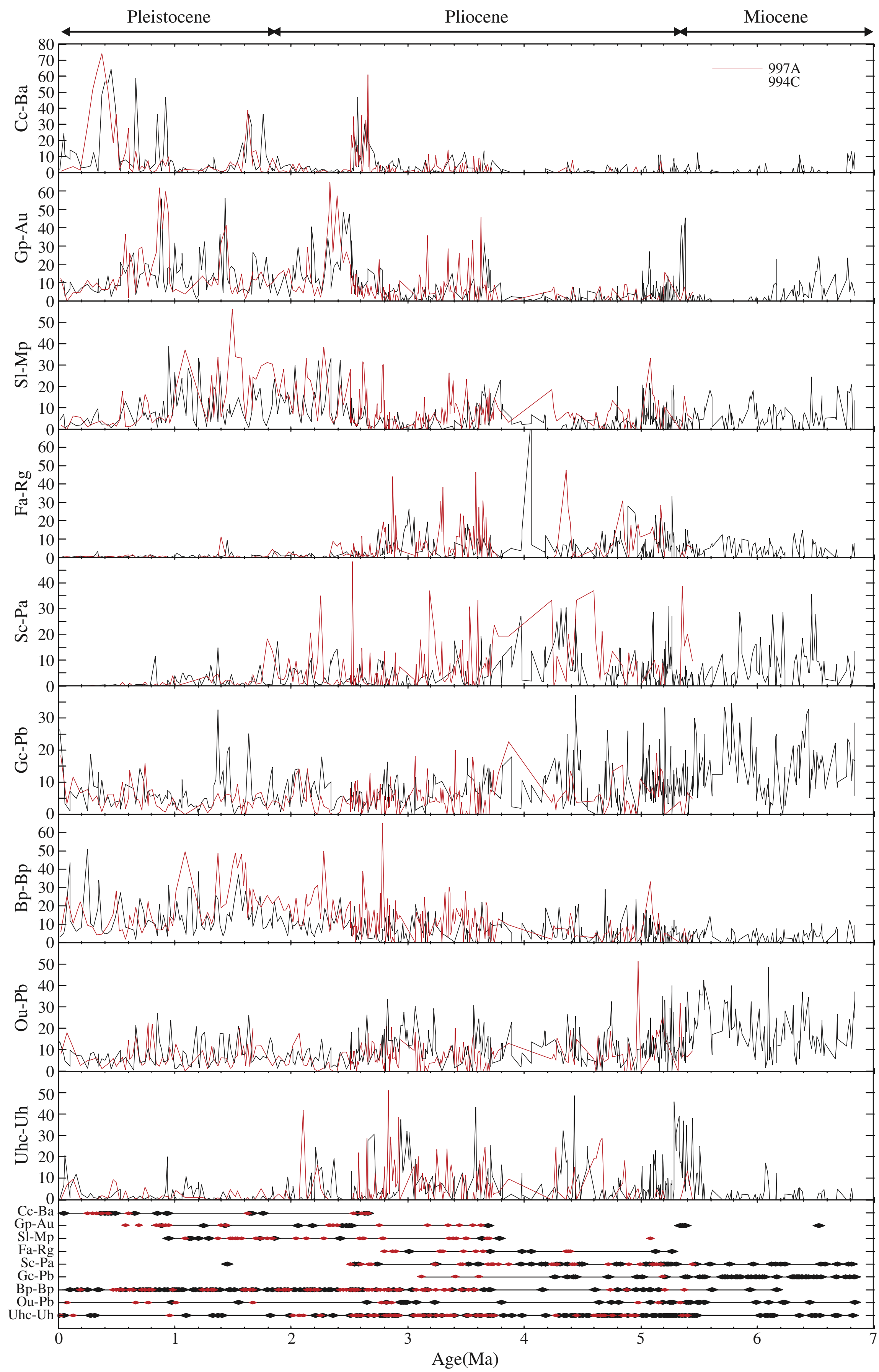

Fig. 3. Benthic foraminiferal biofacies plotted against age and combined with cumulative percentages of major species of each biofacies at Holes 994C (black) and 997A (red). Full forms of each abbreviated biofacies are given in Table 1.

Table 2
Inferred ecological preferences of different benthic foraminifera used in the present study.

Benthic foraminifer species	Ecological preferences
Astrononion umbilicatulum	Not conclusive: associated with high and sustained organic flux (Hald and Korsun, 1997; Gupta and Thomas, 1999; Gupta et al., 2006a,b), alternatively with low primary productivity, well ventilated water column and high salinity (Singh and Gupta, 2004). Possibly, like *Melonis*, using refractory organic carbon (Caralp, 1989); other *Astrononion* species are generally thought to be shallow infaunal (Rasmussen et al., 2002).
Bolivina paula *Bolivina pseudopunctata*	Species of Bolivinids in general indicate dysoxic, organic-rich environments (Sen Gupta and Machain-Castillo, 1993;Wefer et al., 1994; Hill et al., 2003). Common on continental margins, e.g. under WBUS in southern Atlantic (de Mello e Sousa et al., 2006).
Bulimina alazanensis	Organically enriched environments, possibly oxygen depleted (Sen Gupta and Machain-Castillo, 1993; Rathburn and Corliss, 1994; Gooday, 2003). Used as a proxy for NADW flux and treated as a "warm benthos fauna" restricted to interglacial stages (Schmiedl and Mackensen, 1997).
Cassidulina carinata	Opportunistic taxon (Nees and Struck, 1999). *C. carinata* and *Gyroidinoides nitidula* association indicative of intermediate organic flux and intermediate to high seasonality (Gupta and Thomas, 2003), may survive at low oxygen (Jorissen et al., 2007).
Cibicides bradyi	Not conclusive: said to be intolerant to low oxygen conditions (Denne and Sen Gupta, 1991; Barmawidjaja et al., 1992), and associated with well-oxygenated deep water with low organic flux and high seasonality (Singh and Gupta, 2004). In contrast, pore patterns and rounded periphery of the test said to indicate adaptation to lower oxygen levels (Rathburn and Corliss, 1994). Co-occurrence with *Bolivina* species suggests tolerance to lower oxygen levels and also occurs with bolivinids on southern Atlantic continental margin (de Mello e Sousa et al., 2006).
Fursenkoina fusiformis	Opportunistic (Alve, 1999; Rasmussen et al., 2002), tolerant to low oxygen and survive in anoxia (Alve, 1994; Bernhard and Alve, 1996; Gustafsson and Nordberg, 2001); abundant in cold-seep environments (Rathburn et al., 2000).
Globobulimina pacifica	Deep-infaunal dwelling, low oxygen and high organic carbon environment (Sen Gupta and Machain-Castillo, 1993; Gooday, 2003); more abundant in sediments with refractory, more degraded organic matter (Schmiedl et al., 2000); may be indicative of laterally transported, partially degraded organic matter (Fontanier et al., 2005).
Globocassidulina subglobosa	Cosmopolitan species, oligotrophic (Singh and Gupta, 2004 and references therein); abundance related to increased vigor of bottom currents (Schmiedl et al., 1997; Rasmussen et al., 2002; Smart et al., 2007).
Globocassidulina tumida	Not well known. *Globocassidulina* species are common in regions where organic carbon flux is very high throughout the year (Singh and Gupta, 2004), and have higher abundance in the area of increased bottom water currents (Schmiedl et al., 1997; Rasmussen et al., 2002; Smart et al., 2007).
Gyroidinoides cibaoensis	Low oxygen (Gupta and Thomas, 1999; Gupta et al., 2008), food limited or pulsed food supply (Mackensen et al., 1995; De Rijk et al., 1999), oligotrophic (Singh and Gupta, 2004).
Gyroidinoides nitidula	Resembling *G. orbicularis*, found in a food limited environment (Singh and Gupta, 2004 and references therein).
Melonis pompilioides	Moderate productivity and intermediate seasonality (Gupta and Thomas, 2003 and references therein), refractory organic carbon (Caralp, 1989; Fontanier et al., 2005).
Nonionella auris	Survives low oxygen, even anoxic conditions, occurs H2S-containing sediments, cold-seep environments, feed on bacteria (Wefer et al., 1994); generally abundant under high productivity (Gooday, 2003). Some *Nonionella* species (*N. stella*) have been reported to grow fast under very high productivity (Corliss and Silva, 1993), even at low oxygen conditions (Bernhard et al., 1997).
Oridorsalis umbonatus	Cosmopolitan, very long-lived taxon (Gupta and Thomas, 1999). Well oxygenated, low organic carbon environment (Mackensen et al., 1985; Gooday, 2003), organic food limited and low oxygen (Rathburn and Corliss, 1994). Probably environmentally flexible, occurs over wide depth range and age range (since Late Cretaceous), (Kaiho, 1998). Association with *P. bulloides* indicates they can survive with low oxygen and intermediate to high organic carbon rich environment.
Pullenia bulloides	Intermediate flux of organic matter, poorly ventilated deep waters (Rathburn and Corliss, 1994). An assemblage of *P. bulloides* and *Cassidulina teretis* indicates high sediment organic carbon (Mackensen et al., 1985).
Pullenia quinqueloba	High organic matter (Schnitker, 1986) and deposit feeder (Liu et al., 1997).
Pyrgo lucernula and *Quinqueloculina weaveri*	Member of miliolids may prefer cool, oligotrophic, well-oxygenated bottom water conditions (Mackensen et al., 1995; Altenbach et al., 1999; Jorissen, 1999; Schmiedl et al., 2000; Rasmussen et al., 2002; Gooday, 2003; Gupta and Thomas, 2003). *Quinqueloculina* and *Pyrgo* are also reported in seep environments (Robinson et al., 2004). Some species of miliolids (e.g. *Articulina* spp.) are associated with more oxygenated conditions during recovery from low oxygen [e.g. Mediterranean sapropels, (Mullineaux and Lohmann, 1981; Jorissen, 1999)].
Robulus gibbus	Not well constrained. Infaunal (Corliss, 1991), another species of this genus, *R. iota* is a characteristic of oxygen minimum zones (Hermelin and Shimmield, 1990).
Sphaeroidina bulloides	Well-oxygenated (Gupta and Thomas, 1999), high productivity (Gooday, 2003). May tolerate low oxygen condition (Hermelin and Shimmield, 1990).
Uvigerina hispida	In general uvigerinds show close affinity with high productivity independent of bottom water oxygenation (Lutze, 1986; Rathburn and Corliss, 1994). *U. hispida* shows higher abundance in low oxygen, high organic carbon rich environment, indicates period of erosion and downward transportation (McDougall, 1996).
Uvigerina hispido-costata	*U. hispido-costata* is abundant in high organic carbon flux, low oxygen settings (Gupta and Thomas, 2003; Murgese and Deckker, 2005).
Uvigerina peregrina	*Uvigerina peregrina* is more closely related to the continuous organic carbon flux than to the oxygen minima (Rathburn and Corliss, 1994), association of *U. peregrina* with *B. aculeata*, *C. bradyi*, *U. hispida* and *U. proboscidea* indicates presence of NADW (Murray, 2006).
Dentalina stimulea *Frondicularia advena* *Glandulina laevigata* *Nodosaria longiscata* *Pleurostomella alternans* *Stilostomella consobrina* *Stilostomella lepidula*	This group belongs to the elongated benthics community and disappears during the last global extinction (mid Pleistocene transition) except *Glandulina laevigata*. Moderately deep infaunal, tolerant of low oxygen (Gupta, 1993) and wide range of bottom water temperature and dissolve oxygen (Hayward et al., 2007), found in oligotrophic and eutrophic region with sustained or highly seasonal phytoplankton productivity, tolerant of changes in the quantity or seasonality of organic carbon (Hayward et al., 2010a).

possible to identify significant associations of species. We identified nine biofacies (Table 1), indicated by the abbreviated names of their dominant species. We recognized: 1. Uhc–Uh (dominant species: *Uvigerina hispido-costata*, *Uvigerina hispida*, *Uvigerina peregrina* and *Globocassidulina tumida*), 2. Sc–Pa (dominant species: *Stilostomella consobrina*, *Pleurostomella alternans*, *Nodosaria longiscata* and *Dentalina stimulea*), 3. Gc–Pb (dominant species: *Gyroidinoides cibaoensis*, *Pullenia bulloides*, *Cibicides bradyi*, *Gyroidinoides nitidula*, *Sphaeroidina bulloides*, *Quinqueloculina weaveri* and *Globocassidulina subglobosa*), 4. Fa–Rg (dominant species: *Frondicularia advena*, *Robulus gibbus* and *Glandulina laevigata*), 5. Ou–Pb (dominant species: *Oridorsalis umbonatus* and *P. bulloides*), 6. Bp–Bp (dominant species: *Bolivina pseudopunctata*, *Bolivina paula*, *Fursenkoina fusiformis*, *C. bradyi*, *Pyrgo lucernula*, *Stilostomella lepidula* and *Nonionella auris*), 7. Sl–Mp (dominant species: *S. lepidula*, *Melonis pompilioides*, *Astrononion umbilicatulum* and *Pleurostomella alternans*), 8. Cc–Ba (dominant species: *Cassidulina carinata* and *Bulimina alazanensis*) and 9. Gp–Au (dominant species: *Globobulimina pacifica*, *Astrononion umbilicatulum* and *Pullenia quinqueloba*). All species in biofacies 2 (Sc–Pa) are elongate cylindrical species, as is *S. lepidula* (Fig. 3).

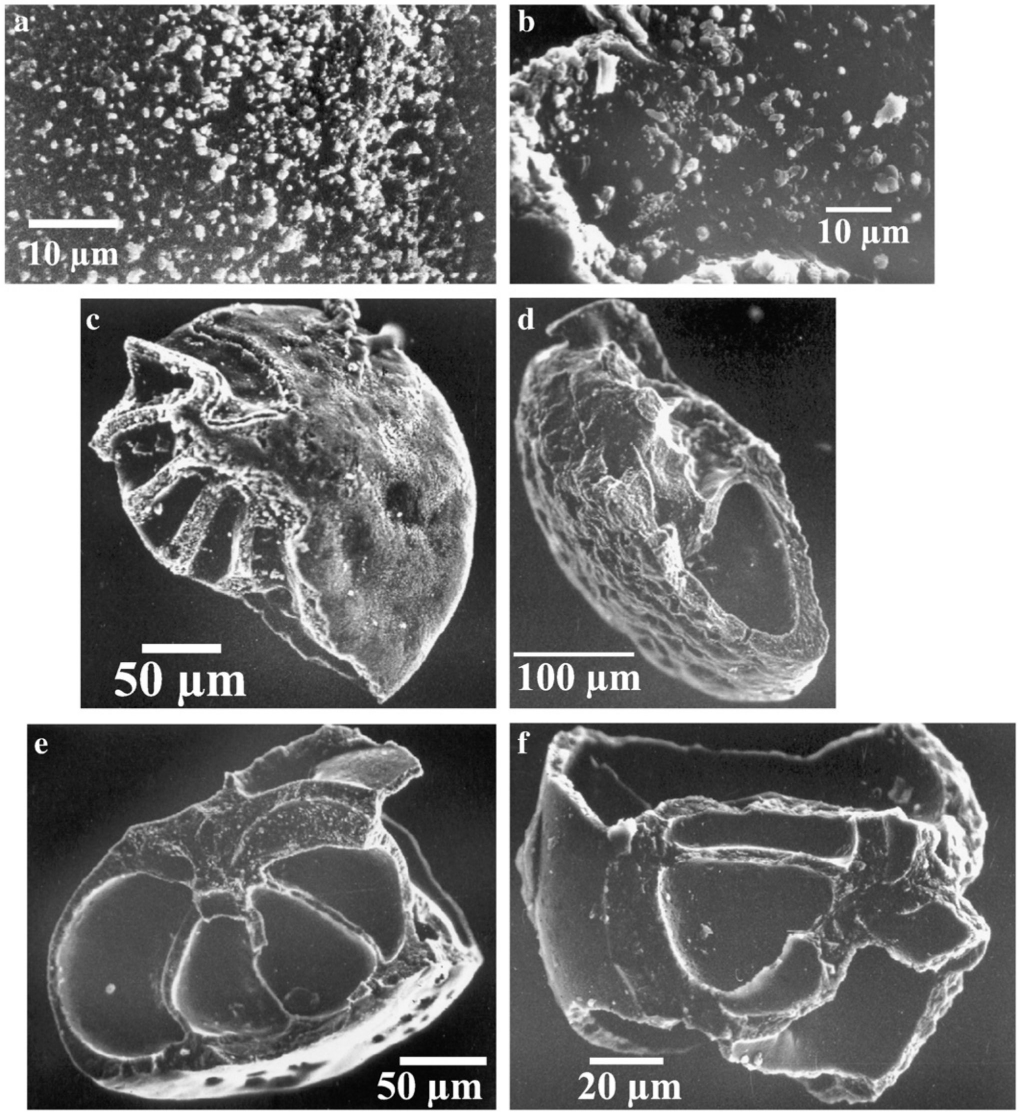

Fig. 4. SEM photographs of broken specimens taken from Hole 994C. Photographs (a) and (b) contain cryptocrystalline granular growth inside the tests of *Cibicides bradyi* (depth 247.43 mbsf, age 3.52 Ma) and *Oridorsalis umbonatus* (depth 458.1 mbsf, age 5.08 Ma), respectively. Photographs (c) to (f) represent overgrowth free benthic foraminiferal tests. Photographs (c) and (d) are of *Cibicides wuellerstorfi* (depth 41.15 mbsf, age 0.93 Ma and 700.42 mbsf, 6.82 Ma, respectively), (e) is of *C. bradyi* (depth 28.66 mbsf, age 0.7 Ma) and (f) is of *O. umbonatus* (depth 159.15 mbsf, age 2.71 Ma). All isotopic values are calibrated to *Cibicides wuellerstorfi*.

Over the full studied interval, the benthic foraminiferal assemblages are typical of continental margin regions, with common species indicative of a fairly high food supply, possibly mixtures of more labile, locally produced organic matter and laterally transported, more refractory organic material (e.g., Fontanier et al., 2005; de Mello e Sousa et al., 2006; Jorissen et al., 2007; Thomas, 2007). The sites were probably influenced by a fairly high but fluctuating food supply, with the Ou–Pb biofacies indicative of the somewhat lower productivity periods, the Uhc–Uh and Bp–Bp biofacies indicative of more productive intervals.

Biofacies Ou–Pb and Uhc–Uh are present throughout the studied interval, with the highest abundances of Ou–Pb before 5 Ma, and those of Uhc–Uh between 5.3 and 2 Ma. Biofacies Bp–Bp was present throughout the studied interval, but at significant values only after 6.2 Ma, and it increased in abundance after 5 Ma and again after 1.8 Ma. Biofacies Fa–Rg was overall rare, but least so between 5.2 and 2.6 Ma. Biofacies Gp–Au and Sl–Mp became common at 3.8–3.7 Ma, Cc–Ba at 2.7 Ma. Biofacies Sc–Pa and Gc–Pb (in Hole 994C) became much less abundant at 2.5 and 3.1 Ma, respectively, Gp–Au and Sl–Mp at 0.8 and 1.0 Ma, respectively (Fig. 3).

There was a major faunal turnover in the interval between 3.8 Ma and 2.5 Ma: Biofacies Sl–Mp, Gp–Au, and Cc–Ba replaced biofacies Gc–Pb, Sc–Pa and Fa–Rg. A smaller turnover occurred at 1.0–0.8 Ma. The data on overall turnover in benthic assemblages from this sediment drift on a continental margin resemble data from open ocean sites and other oceans, in that we see a disappearance of elongate species with a complex aperture at times of increased intensity of glaciation (e.g., Kawagata et al., 2005; Hayward et al., 2010a,b). There is no overall clear change in assemblages indicative of a major increase or decrease in food supply over the studied interval, although the type of organic matter may very well have changed over time, as indicated by the turnover in biofacies (Tables 1, 2; see below).

3.2. Geochemical data

3.2.1. Diagenetic effects

The samples studied were deposited over a large burial range, with the lowermost samples in Hole 994C now at about 700 mbsf (Fig. 2).

Table 3
List of broken species from different samples from Hole 994C with corresponding depth, age and isotopic values used to understand authigenic carbonate growth.

Name of the specimen	Sample no.	Depth (m)	Age (Ma)	$\delta^{13}C$ ‰	$\delta^{18}O$ ‰	Authigenic calcite
Bolivina paula	2H-3, 75–77	8.15	0.25			No
Oridorsalis umbonatus	4H-4,76–78	28.66	0.7	0.88	3.72	No
Cibicides bradyi	4H-4,76–78	28.66	0.7			No
Cibicides wuellerstorfi	4H-4,76–78	28.66	0.7			No
Cibicides bradyi	5H-6, 75–77	41.15	0.93	−2.61	4.9	No
Cibicides wuellerstorfi	5H-6, 75–77	41.15	0.93			No
Epistominella exigua	5H-6, 75–77	41.15	0.93			No
Oridorsalis umbonatus	10H-1, 75–77	72.65	1.35	0.97	3.47	No
Cibicides wuellerstorfi	10H-1, 75–77	72.65	1.35			No
Epistominella exigua	10H-1, 75–77	72.65	1.35			No
Oridorsalis umbonatus	10H-5,74–76	78.64	1.43	0.93	4.49	No
Cibicides bradyi	10H-5,74–76	78.64	1.43			No
Oridorsalis umbonatus	20X-1, 75–77	159.15	2.71	−1.53	4.09	No
Cibicides bradyi	20X-1, 75–77	159.15	2.71			No
Cibicides kullenbergi	26X-2, 71–73	215.11	3.23	−1.92	3.89	No
Oridorsalis umbonatus	26X-2, 71–73	215.11	3.23			No
Oridorsalis umbonatus	30X-CC, 50–52	247.43	3.52	0.76	3.21	No
Cibicides bradyi	30X-CC, 50–52	247.43	3.52			Yes?
Gyroidinoides cibaoensis	30X-CC, 50–52	247.43	3.52			No
Bolivina paula	30X-CC, 50–52	247.43	3.52			No
Cibicides bradyi	40X-2, 52–54	330.3	4.16	1.11	3.12	No
Cibicides wuellerstorfi	40X-2, 52–54	330.3	4.16			No
Epistominella exigua	40X-2, 52–54	330.3	4.16			No
Oridorsalis umbonatus	56X-CC, 0–2	458.1	5.08	−1.53	3.61	Yes?
Hoeglundina elegans	56X-CC, 0–2	458.1	5.08			No
Cibicides wuellerstorfi	84X-5, 69–71	700.42	6.82	−1.96	2.96	No
Robulus gibbus	84X-5, 69–71	700.42	6.82			No

There is considerable evidence for recrystallization of material in the holes, and the presence of gas hydrates shows that diagenesis of the sediments has been fairly intensive, at least in some depth intervals. The first question we need to answer thus is whether the benthic foraminiferal stable isotope values reflect the environment of deposition of the sediments or the downhole diagenesis.

We examined specimens of benthic foraminifera using Scanning Electron Microscopy, breaking specimens to evaluate whether diagenetic calcite was commonly present. Although most specimens show at least some recrystallization, we found no evidence for severe overgrowth in most specimens investigated. The exceptions are a few specimens of *Cibicides bradyi* (3.52 Ma) and *Oridorsalis umbonatus* (5.08 Ma), showing calcite overgrowths inside their tests (Fig. 4). The overgrowths appear to be cryptocrystalline and patchily distributed, and do not resemble the authigenic calcite shown in SEM micrographs by Millo et al. (2005). The $\delta^{13}C$ values of *Cibicides wuellerstorfi* from these two samples are 0.76‰ and −1.53‰, i.e., they are isotopically heavier than samples without overgrowth (Table 3). The $\delta^{13}C$ and $\delta^{18}O$ values of diagenetic calcite from Hole 994C (Pierre et al., 2000) do not show a significant correlation with the carbon and oxygen isotopic values of benthic foraminifera from the same levels (Fig. 5). The plot of $\delta^{18}O$ vs. TOC values shows a significant negative correlation ($R = -0.5$), and there is no significant correlation between $\delta^{13}C$ and TOC values.

We compared our benthic foraminiferal isotope records with the data in the global compilation of Zachos et al. (2001) (Fig. 6a) and Cramer et al. (2009) (Fig. 6b), as well as with those from a short time interval at close-by Site 1058 (Franz and Tiedemann, 2002). By far most values in our $\delta^{18}O$ records are within the variability of the data presented by these two groups of authors, with only a few exceptions. We excluded some extreme data points that differ by more than 0.5‰ from the compilation (indicated by bold, Appendix 3). The $\delta^{13}C$ values for most samples in our records overlap the range of values in Zachos et al. (2001), being between −1.5‰ and +1‰. We excluded the few values outside this range from further analysis (bold face, Appendix 3). For some time intervals (see below), our values are significantly lower (1 to 3%) than the coeval values in the records in Zachos et al. (2001), although still within the −1.5‰ to +1‰ range. These lower values overlap with values for SCW values as shown in Franz and Tiedemann (2002) and Poore et al. (2006).

Our data are less similar to the values published by Cramer et al. (2009) for various ocean basins, but are closest to these authors' data from the Southern North Atlantic (Fig. 6b). Neither Zachos et al. (2001) nor Cramer et al. (2009) include data from BOR. The lower $\delta^{13}C$ values in our records, which overlap with values for Southern Component Waters in Franz and Tiedemann (2002) and Poore et al. (2006) occur at earlier times (i.e., back to the beginning of our records at 7 Ma) than in the compiled records of Zachos et al. (2001) and Cramer et al. (2009) (Fig. 6a,b), indicating that such SCW occurred in the westernmost North Atlantic Basin over the whole period studied, in contrast with other locations.

We thus argue that our records overall reflect paleoceanographic conditions rather than diagenetic processes, with the more negative values of the $\delta^{13}C$ record reflecting mainly SCW, the more positive ones NCW, after excluding some extreme values, which we consider affected by diagenetic processes (Appendix 3; bold face). Our time resolution makes it impossible to draw inferences about changes on glacial–interglacial time scales, and we chose to take 5-point moving averages of the isotope data and TOC to make the overall trends clear (Fig. 7).

3.2.2. TOC and stable isotope data

Total Organic Carbon values at Hole 994C fluctuate, but are generally highest in the lower part of the record (before ~3.6 Ma), with an average of 1.5 (wt%). The values declined until about 1.6 Ma, after which they remained stable at around 0.75 wt %. Comparison of Fig. 3 with Figs. 7 and 8 shows that biofacies Uhc–Uh, Sc–Pa, Gc–Pb, Fa–Rg and Ou–Pb dominated intervals of high TOC, whereas biofacies Bp–Bp, Sl–Mp, Cc–Ba and Gp–Au were dominant during intervals of lower TOC values.

The pattern of TOC is similar (though opposite in sign) to the record of oxygen isotope values of benthic foraminifera: these values

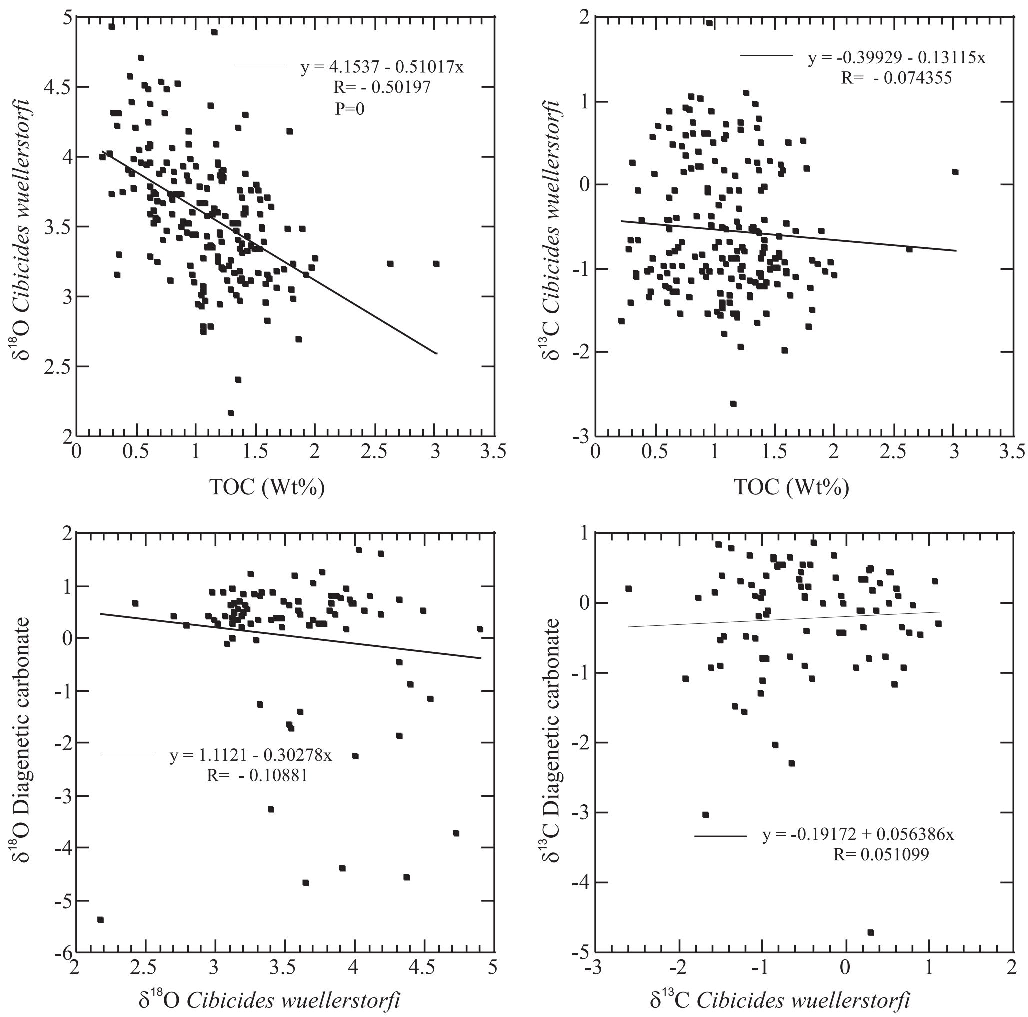

Fig. 5. Values of $\delta^{18}O$ and $\delta^{13}C$ of *C. wuellerstorfi* plotted versus TOC and versus carbon and oxygen isotopic values of diagenetic carbonate at Hole 994C (Pierre et al., 2000).

fluctuated around 3.25‰ before about 3.6 Ma, then increased until about 1.6 Ma, and afterwards fluctuated around a value of about 4‰. There thus is a clear, negative correlation between these two parameters (Fig. 5). Our records are not of sufficient time resolution to document the details of the glacial–interglacial variability over the time period investigated, but document the overall well-known record of intensification of NHG, and show that this increased glaciation was linked to decreasing deposition of TOC at BOR.

The benthic carbon isotope values are not significantly correlated to TOC and $\delta^{18}O$ values (Fig. 5) of diagenetic carbonate. The record shows great variability, but overall high values (>−0.5‰) between 5.0 and 3.6 Ma, between 2.4 and 1.2 Ma, and between 0.8 Ma and the last few ten thousands of years (Fig. 7). The relative abundance of *Cibicides wuellerstorfi* shows overall higher values (>10%) in intervals with higher $\delta^{13}C$ values (Figs. 7, 8).

4. Discussion

The climate of the Earth has cooled over the last 7 Ma (e.g., Zachos et al., 2001), with significant build up of ice on Southern Greenland in the late Miocene (Maslin et al., 1998; Haug et al., 2005), but global cooling was interrupted by warm phases such as the early Pliocene (e.g., Wara et al., 2005; Pagani et al., 2010), during which transient changes occurred in the size in Antarctic ice sheets (e.g., Pollard and deConto, 2009). Overall, however, there has been a net increase in polar ice volume since the late Miocene, and an increase in the magnitude of glacial–interglacial variability, with the 100 kyr eccentricity-forced component of orbitally-driven glacial–interglacial climate variability dominant over the last 800–900 kyr (e.g., Gupta et al., 2001; Haug et al., 2005).

In the North Atlantic, the production of the NCW was strongly enhanced during the Pleistocene warm interglacial intervals (e.g., Reynolds et al., 1999; Frank et al., 2002; Franz and Tiedemann, 2002; Hagen and Keigwin, 2002; Lynch-Stieglitz et al., 2007; Evans and Hall, 2008). During glacial intervals, in contrast, the upper boundary between SCW and the glacial equivalent of NADW [GNAIW; (Lynch-Stieglitz et al., 2007)] shoaled by more than 2200 m along BOR (Franz and Tiedemann, 2002; Evans and Hall, 2008). Less is known of the variability in NCW/SCW for earlier periods.

The $\delta^{13}C$ values of *Cibicides wuellerstorfi* have been widely used to detect changes in deep-water ventilation in the Atlantic and between oceans (e.g., Haug and Tiedemann, 1998). In general, $\delta^{13}C$ values of benthic foraminiferal tests (commonly *Cibicides* spp.) which calcified within the poorly-ventilated, nutrient-rich SCW are more depleted in $\delta^{13}C_{DIC}$, with values between 0 and −1‰. Tests calcified within NCW are relatively enriched, with values >0‰ (Kroopnick, 1985; Raymo et al., 1998; Franz and Tiedemann, 2002; Curry and Oppo, 2005; Lynch-Stieglitz et al., 2007; Ravelo and Hillaire-Marcel, 2007). Very large fluctuations in $\delta^{13}C$ values thus are seen at locations where SCW alternated with NCW (e.g., Franz and Tiedemann, 2002).

Due to the time resolution of our study we cannot make inferences about changes on glacial–interglacial time scales, but the carbon isotope and *Cibicides wuellerstorfi* % data (Fig. 8) indicate that our sites were dominantly covered by SCW (characterized by low $\delta^{13}C$ values and low % of *C. wuellerstorfi*) between 7 and 5 Ma (late Miocene–earliest Pliocene), with $\delta^{13}C$ values below those in the Zachos et al. (2001) curves (Fig. 6), and overlapping with SCW values in Poore et al. (2006). Calcareous nannoplankton and diatom assemblages (Ikeda et al., 2000; Okada, 2000) indicate fairly high productivity at that time, in agreement with dominance by benthic foraminiferal biofacies (biofacies Gc–Pb, Sc–Pa and Uhc–Uh), indicative of a high and probably not highly seasonal food supply, with possible current influence. The overlying surface waters were probably mainly gyre-margin environments, with some upwelling of the nutrient-enriched SCW, which reached a few km depth (Ikeda et al., 2000; Okada, 2000). This interval in the late Miocene and earliest Pliocene was characterized by the presence of a western as well as eastern Antarctic ice sheet (e.g. Zachos et al., 2001; Cramer et al., 2009), so that the volume of SCW may have been high due to cooling at high southern latitudes, whereas NCW volume may have been limited by the relatively shallow depth of the sill in the northernmost Atlantic over which these NCW waters flow in the Atlantic Ocean (Wright and Miller, 1996; Poore et al., 2006).

Between about 5.0 and 3.6 Ma the sites were mainly under the influence of NCW, with benthic $\delta^{13}C$ values of up to 1.25‰. During this period the diatom and nannofossil productivity declined (Fig. 8), although the TOC in the sediments shows a moderate change only. The benthic foraminiferal biofacies underwent minor changes only, with the more common presence of biofacies Fa–Rg, possibly indicative of a somewhat lower food supply, or possibly somewhat less labile, more refractory organic matter, possibly also leading to the somewhat increased abundance of biofacies Bp–Bp. This organic matter might have arrived by lateral transport of the vigorous WBUC, with higher current intensity indicated by the higher % of *Cibicides wuellerstorfi* (Figs. 7, 8). Possibly, the younger NCW brought fewer nutrients to BOR, resulting in lesser primary productivity at the surface, or the gyre location shifted, bringing more oligotrophic waters over the BOR during the warm early Pliocene (Wara et al., 2005; Dowsett et al., 2009; Seki et al., 2010). This overall warm period thus may have seen Atlantic MOC similar to that of the present day, with large volume NCW production, relatively low primary productivity in water overlying BOR. NCW may have formed at a similar

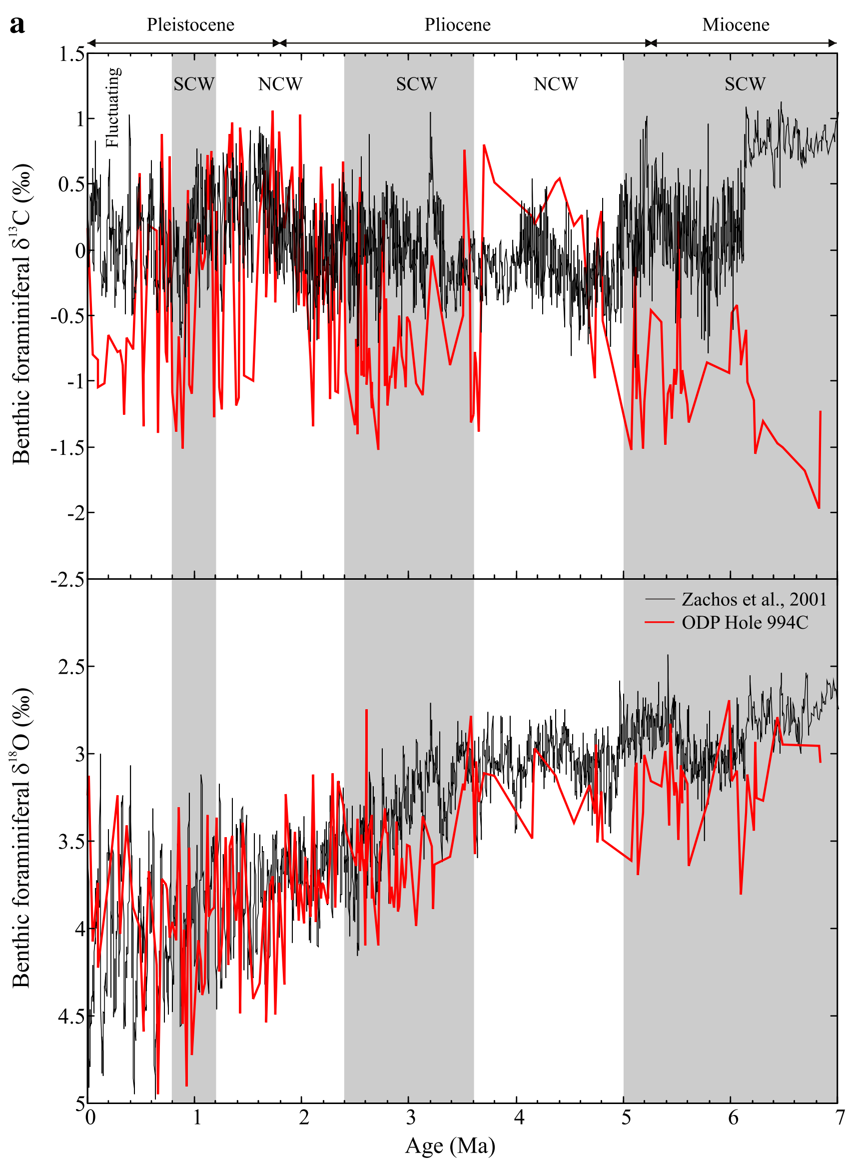

Fig. 6. a: Benthic oxygen and carbon isotope values of Hole 994C compared to the global compilation of Zachos et al. (2001). Gray bars indicate inferred times of SCW and NCW dominance at the sites. b: Benthic oxygen and carbon isotope values of Hole 994C compared to the compilation of Cramer et al. (2009) from South Atlantic and Northern part of the Southern Ocean. Gray bars indicate inferred times of SCW and NCW dominance at the sites.

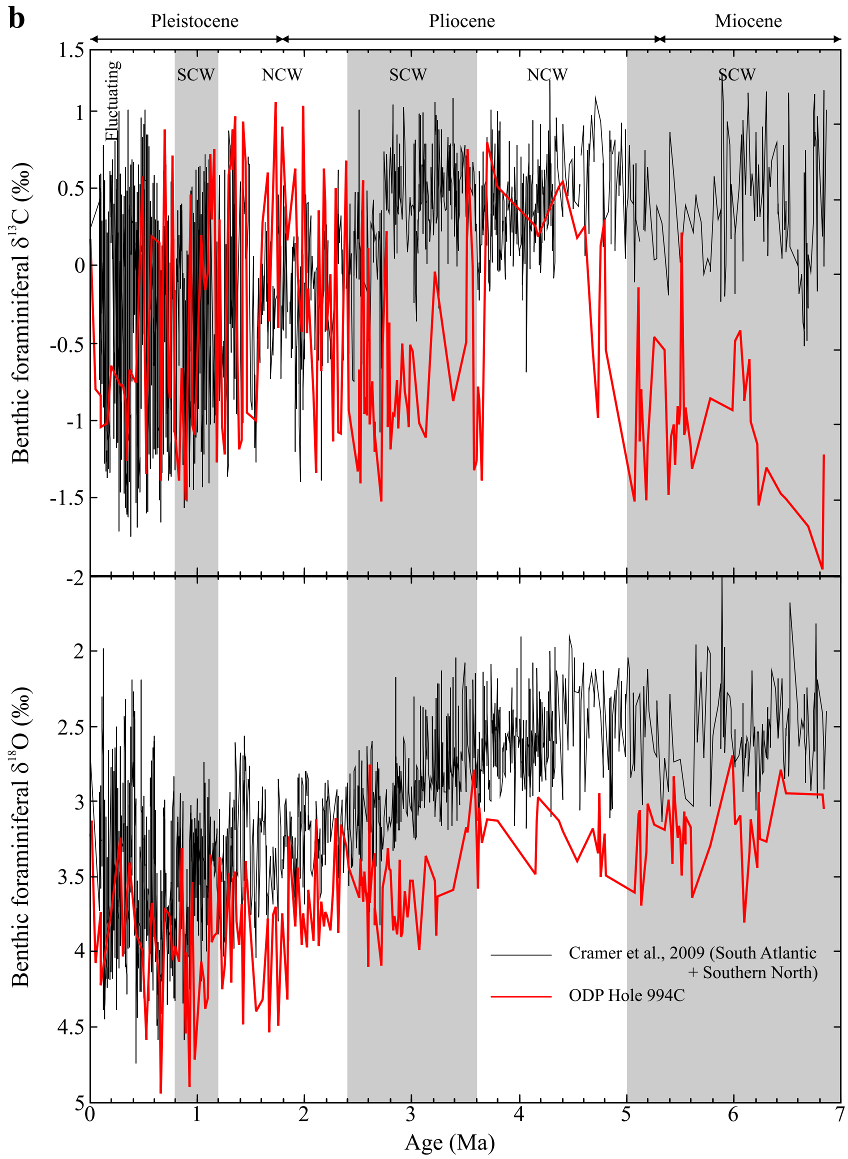

Fig. 6 (*continued*).

location as today's NADW, i.e. relatively further North than during colder intervals, and in addition the elevation of the sill where these waters flow into the Atlantic Ocean to form the WBUC may have been lowered (Wright and Miller, 1996; Poore et al., 2006).

The period between 3.6 and 2.4 Ma saw a return of SCW to the sites, with benthic δ^{13}C values between −1 and −1.5‰. This was the time of major intensification of the Northern Hemisphere Glaciation (Haug and Tiedemann, 1998; Zachos et al., 2001; Mudelsee and Raymo, 2005), as indicated at our sites by increasing benthic δ^{18}O values, as well as declining TOC values. The decline in TOC values was likely not simply related to the change in dominant deep-water mass over the sites, since the change from SCW to NCW at about 5 Ma did not have a significant effect on TOC. This interval also saw a decline in depth of the Iceland–Greenland sill (Poore et al., 2006), possibly limiting the volume on NCW. This interval also saw the largest turnover of benthic biofacies, with the decrease in Fa–Rg (low to intermediate food supply), Sc–Pa (low to intermediate food, extinction group species), and Gc–Pb (intermediate-high food flux), and the increase in biofacies Bp–Bp (high organic carbon), Sl–Mp (intermediate-refractory food), Gp–Au (high food supply, possibly refractory), and Cc–Ba (intermediate food flux, possibly seasonal). There thus may have been an overall further increase in the flow of more refractory organic carbon to the sites (dominance of biofacies Sl–Mp), combined with a more seasonal food flux. The primary productivity of diatoms and calcareous nannoplankton increased once more, similar to its status at 7.0–5.0 Ma, whereas TOC started to decline, in contrast to that earlier period. Possibly, less of the more labile organic matter reached the sea floor, even with the presence of the less-ventilated SCW, with a change to more refractory and more seasonal food supply. It is also possible that the cooling resulted in increasingly vigorous bottom currents (continuing into the following time periods), leading to less deposition of fine-grained organic material from higher northern latitudes, although this is not confirmed by the overall low abundance of *Cibicides wuellerstorfi*.

The biofacies which decreased at this time include typical 'extinction group' species (Kawagata et al., 2005; Hayward et al., 2010a,b), which became extinct globally during the late Pleistocene cooling of the deep-sea. These species all have complexly structured apertures, suggesting that they may have shared a mode of feeding which no longer exists in the cold, well-ventilated oceans of the Present (Hayward et al., 2010a,b). They may have fed on a phytoplankton source which became extinct during the taxonomic

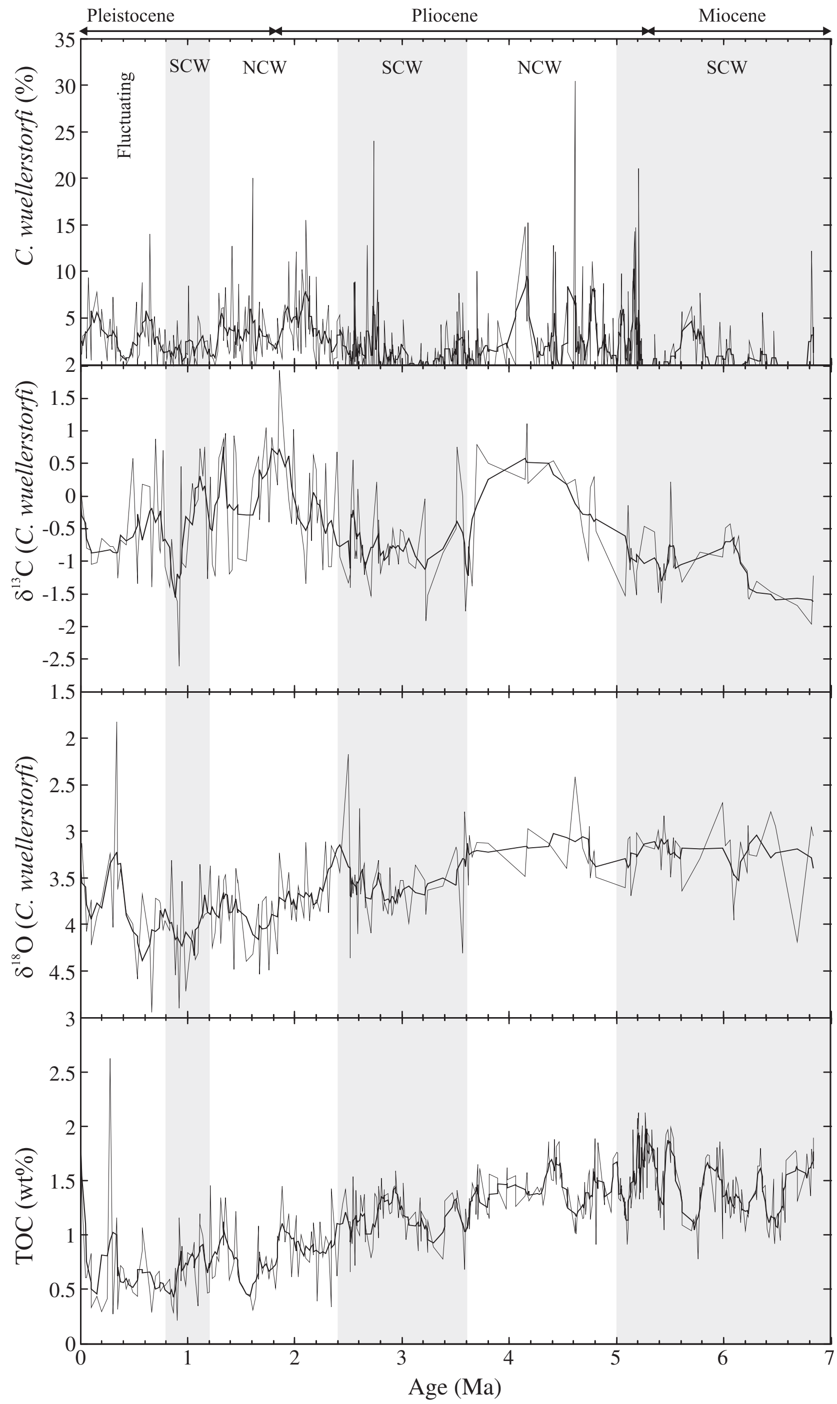

Fig. 7. Values of TOC, $\delta^{18}O$ and $\delta^{13}C$ of *C. wuellerstorfi* at Hole 994C and relative abundance of *C. wuellerstorfi*, with interpretation of the presence of Southern and Northern Component Waters over the sites. Thick lines represent 5 point moving average.

turnover of phytoplankton of this period (Ikeda et al., 2000; Okada, 2000), or on prokaryotes, the metabolic rates of which slowed down due to declining temperatures (Hayward et al., 2010a,b).

Waters over the sites were dominated by NCW between 2.4 and 1.2 Ma, a period which saw fairly stable benthic foraminiferal assemblages, despite the change in dominant water mass. In contrast to the period of NCW between 5.0 and 3.6 Ma, this period saw persistent high productivity by diatoms and nannofossils, but TOC remained low. Possibly, the gyre margin remained over the sites. The surface water circulation in the western North Atlantic may have differed from that during the earlier NCW-period, because of the shoaling of the Panamanian isthmus at around 4.6 Ma (Haug and Tiedemann, 1998), strengthening the Gulf Stream, thus keeping the gyre margin further out.

Between 1.2 and 0.8 Ma the SCW returned over the sites, with persistent high productivity of calcareous nannofossils and diatoms, possibly explaining the high abundance of biofacies Bp–Bp. Towards the end of this period climate variability increased, with the establishment of the dominant 100 kyr variability (e.g., Maslin et al., 1998; McClymont and Rosell-Melé, 2005). Benthic assemblages underwent additional turnover during this period, with a decrease in biofacies Sl–Mp (intermediate-refractory food), Gp–Au (high food

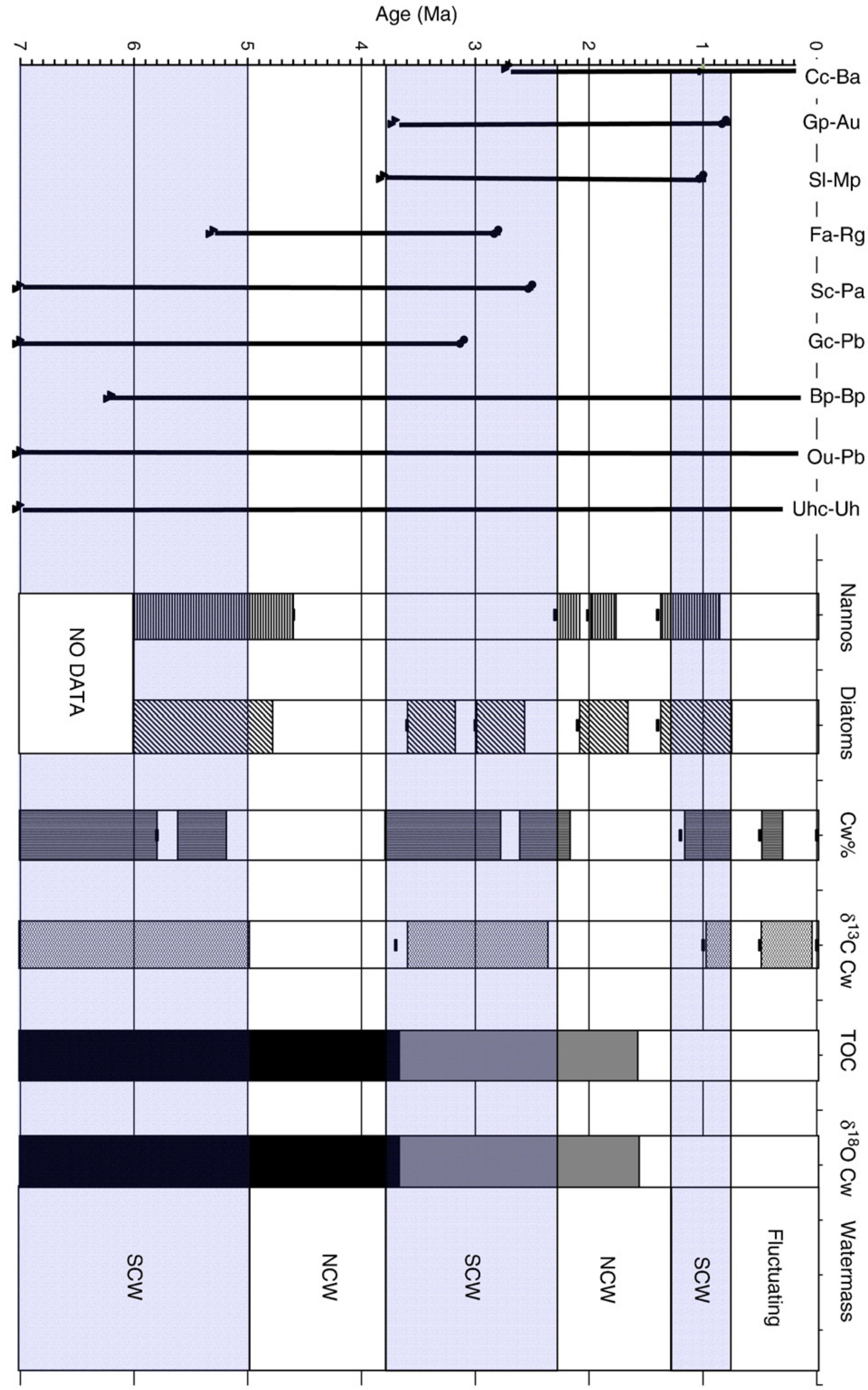

Fig. 8. Comparison of the most abundant occurrence of the 9 biofacies (indicated by vertical lines labeled with name of biofacies), high productivity periods as indicated by diatoms (Ikeda et al., 2000) and calcareous nannoplankton (Okada, 2000) with periods of high productivity marked by horizontal lines (nannofossils) and slanted lines (diatoms), relative abundance of *C. wuellerstorfi* (Cw%), with low abundances marked by vertical lines, high and low values of $\delta^{13}C$ of *C. wuellerstorfi* ($\delta^{13}C$ Cw, low values marked by wavy lines), TOC (black bar indicates interval of high values, followed by gray indicating gradual transition to lower values), and $\delta^{18}O$ of *C. wuellerstorfi* ($\delta^{18}O$ Cw; black bar indicates low values, gray transition into higher values), with interpretation of dominant water masses over BOR at a depth of ~ 2800 m.

supply, possibly refractory). The first of these reflects the regional expression of the global extinction of the cylindrical species, the last of which became extinct at this time (Hayward et al., 2010a,b). The second decline suggests an overall decline in transport of more refractory organic matter to the sites. Such a decline might be linked to increasingly vigorous bottom currents (as argued above), or declining refractory organic matter transported from land due to increasing glaciation and declining vegetation on land in the north (with both NCW and SCW flowing over BOR from the North).

The last 800 kyr is characterized by strongly variable conditions, with declining diatom and nannofossil productivity, and strong fluctuations in NCW–SCW over the sites, due to the high intensity of climate variability at the 100 kyr periodicity, and benthic assemblages were similar to those in present days.

5. Conclusions

Environments of the Blake Outer Ridge at depths of ~2800 m have been alternatively influenced by dominant Northern Component Waters and Southern Component Water over the last 7 Ma. This alternating influence has not been shown clearly in records from other locations in the North Atlantic, probably because these are further away from the Western Boundary Under Current (WBUC), which transport most of the NCW to the South.

The late Miocene through the earliest Pliocene (7–5 Ma) saw the sites mostly covered by SCW, at overall high productivity under a gyre margin. During the warmer early Pliocene (5.0–3.6 Ma) NCW water was present at the sites, SCW was present between 3.6 and 2.4 Ma during the increase of the Northern Hemisphere Glaciation, NCW returned between 2.4 and 1.2 Ma, and SCW between 1.2 and 0.8 Ma, followed by strongly fluctuating conditions. Dominance of NCW or SCW is linked to high latitude climate, with more NCW forming during overall warmer periods, as well as to the elevation of the Greenland–Iceland sill, with lesser elevation leading to larger volumes of NCW.

There is no clear correlation between high primary productivity and presence of NCW/SCW at the site locations, and there is no clear correlation between TOC and primary productivity indicators. Possibly at least some of the organic matter preserved was refractory organic matter from lateral transport or transport from the continental margin.

With increasing Northern Hemisphere Glaciation (3.6–2.4 Ma) the TOC of the sediments declined at the same time as the decline in temperature/increase in ice volume (increasing $\delta^{18}O$ values), even as primary productivity (diatoms, nannoplankton) remained high. Possibly more vigorous currents resulted in declining deposition of refractory, fine-grained organic matter to the seafloor, indicating some decoupling between bentho-pelagic processes.

Benthic biofacies do not show strong changes during times of change in bottom water masses over the sites, and also do not show major changes linked to local/regional primary productivity variability (variability in gyre location, upwelling intensity, nutrient content of upwelling waters).

Benthic foraminiferal assemblages are mainly influenced by globally recognized events, i.e., the last global extinction of benthic foraminifera during the intensification of the Northern Hemisphere Glaciation and the change to a world dominated by high amplitude 100 kyr climate variability. The exact causes of the faunal changes are not clear: they have been linked to stepwise cooling, changing circulation patterns, increased ventilation and changes in oceanic primary productivity and the efficiency of the biological pump.

Supplementary materials related to this article can be found online at doi:10.1016/j.palaeo.2011.02.004.

Acknowledgements

AKG thanks the IODP for core samples for the present study under request number 16030A, B. AKB is thankful to IIT, Kharagpur for providing the infrastructure to pursue the work. ET thanks the NSF for partial funding. The TOC analysis was run in the DST-FIST funded TOC Analysis Laboratory of the Department of Geology & Geophysics, Indian Institute of Technology, Kharagpur. We thank Dr. Mimi Katz, Dr. Bruce Hayward and two anonymous reviewers for the constructive reviews.

Appendix 1. List of high-ranked benthic foraminifera from Holes 994C and 997A used in R-mode Principal Component Analysis and Q-mode cluster analysis

1. *Astrononion umbilicatulum* (Uchio) = *Astrononion umbilicatulum* Uchio, 1952, p. 36, txtfig. 1 — Gupta, 1994, pl. 5, fig. 17.
2. *Awhea tosta* (Schwager) = *Nodosaria tosta* Schwager, 1866, p. 219, pl. 5, fig. 42 — Hayward, 2002, pl. 1. figs. 7, 8.
3. *Bolivina paula* (Cushman and Cahill) = *Bolivina paula* Cushman and Cahill, 1932, Marszalek et al., 1969, fig. 10.
4. *Bolivina pseudopunctata* (Höglund) = *Bolivina pseudopunctata* Höglund, 1947, p. 273, pl. 24, fig. 5, pl. 31, figs. 23, 24 — Sarkar et al., 2009, pl. 2. fig. 2.
5. *Bulimina alazanensis* (Cushman) = *Bulimina alazanensis* Cushman, 1927, p. 161, pl. 25, fig. 4 — Gupta, 1994, pl. 3, fig. 7.
6. *Bulimina costata* (d'Orbigny) = *Bulimina costata* d'Orbigny, 1852, p. 115 — Sarkar et al., 2009, pl. 2, fig. 9.
7. *Cassidulina carinata* (Silvestri) = *Cassidulina laevigata* d'Orbigny var. *carinata* Silvestri, 1896, p. 104, pl. 2, fig. 10 — Gupta, 1994, pl. 2, fig. 10.
8. *Cibicides bradyi* (Trauth) = *Cibicides bradyi* Trauth, 1918, p. 665, pl. 95, fig. 5 — Gupta, 1994, pl. 5, figs. 3, 4.
9. *Cibicides kullenbergi* (Parker) = *Cibicides kullenbergi* Parker, 1953, p. 49, pl. 11, figs. 7, 8 — Gupta, 1994, pl. 5, fig. 5.
10. *Cibicides wuellerstorfi* (Schwager) = *Anomalina wuellerstorfi* Schwager, 1866, p. 258, pl. 7, figs. 105–107 — Gupta, 1994, pl. 5, figs. 8, 9.
11. *Dentalina stimulea* (Schwager) = *Nodosaria stimulea* Schwager, 1866, p. 226, pl. 6, fig. 57 — Hayward, 2002, pl. 2, figs. 34–35.
12. *Eggerella bradyi* (Cushman) = *Verneuilina bradyi* Cushman, 1911, p. 54, pl. 2, text figs. 87a–b — Gupta, 1994, pl. 1, fig. 2.
13. *Epistominella exigua* (Brady) = *Pulvinulina exigua* Brady, 1884, p. 696, pl. 103, figs. 13, 14 — Gupta, 1994, pl. 4, figs. 18, 19.
14. *Frondicularia advena* (Cushman) = *Frondicularia advena* Cushman, 1923, p. 141, pl. 20, figs. 1, 2 — Barker, 1960, pl. 66, figs. 8–12.
15. *Fursenkoina fusiformis* (Williamson) = *Stainforthia fusiformis* (Williamson) = *Bulimina pupoides* d'Orbigny Var. *fusiformis* Williamson 1858, P. 63, pl. 5, figs. 129, 130 — Hermelin and Scott, 1985, pl. 4, fig. 14.
16. *Glandulina laevigata* (d'Orbigny) = *Nodosaria* (*Glandulina*) *laevigata* d'Orbigny, 1826, p. 252, pl 1, figs. 1–4 — Sarkar et al., 2009, pl. 4, fig. 20.
17. *Globobulimina pacifica* (Cushman) = *Globobulimina pacifica* Cushman, 1927, p. 67, pl. 14, fig. 12 — Gupta, 1994, pl. 3, fig. 10.
18. *Globocassidulina obtusa* (Williamson) = *Cassidulina obtusa* Williamson, 1858, p. 69, pl. 6, figs. 143, 144 — Murray, 2006, (as Cassidulina), Fig. 5.3, No. 12.
19. *Globocassidulina subglobosa* (Brady) = *Cassidulina subglobosa* Brady, 1884, p. 430, pl. 54, figs. 17a–c — Gupta, 1994, pl. 2, figs. 17, 18.
20. *Globocassidulina tumida* (Heron-Allen and Earland) = *Cassidulina laevigata* d'Orbigny Var. *tumida* Heron-Allen and Earland 1922, p. 137, pl. 5, figs. 8–10 — Gupta, 1994, pl. 3, figs. 1, 2.
21. *Gyroidinoides cibaoensis* (Bermùdez) = *Gyroidina cibaoensis* Bermùdez, 1949, p. 252, pl. 17, figs. 61–63 — Sarkar et al., 2009, pl. 5, fig. 6.
22. *Gyroidinoides nitidula* (Schwager) = *Rotalia nitidula* Schwager, 1866, p. 263, pl. 7, fig. 110 — Gupta, 1994, pl. 6, fig. 15.
23. *Hoeglundina elegans* (d'Orbigny) = *Rotalia elegans* d'Orbigny, 1826, p. 276, no. 54 — Gupta, 1994, pl. 2, figs. 7, 8.
24. *Melonis barleeanum* (Williamson) = *Nonionina barleeanum* Williamson, 1858, p. 32, pl. 3, figs. 68, 69 — Gupta, 1994, pl. 6, fig. 1.
25. *Melonis pompilioides* (Fichtel and Moll) = *Nautilus pompilioides* Fichtel and Moll 1798, p. 31, pl. 2, figs. a–c — Gupta, 1994, pl. 6, figs. 2, 3.
26. *Nodosaria longiscata* (d'Orbigny) = *Nodosaria longiscata* d'Orbigny, 1846, p. 32, pl. 1, figs. 10–12 — Hayward, 2002, pl. 2, fig. 43.
27. *Nonionella auris* (d'Orbigny) = *Valvulina auris* d'Orbigny, 1839, p. 47, lám. 2, figs. 15–17 — Hayward et al., 2002, pl. 1, figs. 36–38.
28. *Nuttallides umbonifer* (Cushman) = *Pulvinulinella umbonifera* Cushman, 1933, p. 90, pl. 9, fig. 9 — Gupta, 1994, pl. 5, figs. 14–16.

29. *Oridorsalis umbonatus* (Reuss) = *Rotalina umbonata* Reuss, 1851, p. 75, pl. 5, fig. 35 — Gupta, 1994, pl. 6, fig. 11.
30. *Pleurostomella alternans* (Schwager) = *Pleurostomella alternans* Schwager, 1866, p. 238, pl. 6, figs. 79, 80 — Hayward, 2002, pl. 1, figs. 22–24.
31. *Pullenia bulloides* (d'Orbigny) = *Nonionina bulloides* d'Orbigny, 1846, p. 107, pl. 5, figs. 9, 10 — Gupta, 1994, pl. 6, fig. 11.
32. *Pullenia quinqueloba* (Reuss) = *Nonionina quinqueloba* Reuss, 1851, p. 71, pl. 5, fig. 31 — Gupta, 1994, pl. 6, fig. 7.
33. *Pyrgo lucernula* (Schwager) = *Pyrgo lucernula* Schwager, 1866, p. 202, pl. 4, fig. 14 — Barker, 1960, pl. 2, figs. 5, 6.
34. *Quadrimorphina laevigata* (Phelger and Parker) = *Valvulineria laevigata* Phelger and Parker, 1951, p. 25, pl. 13, figs. 11, 12 — Boltovskoy, 1978, pl. 8, figs. 42, 43.
35. *Quinqueloculina lamarckiana* (d'Orbigny) = *Quinqueloculina lamarckiana* d'Orbigny 1839, p. 189, pl. 11, figs. 14–15 — Gupta, 1994, pl. 1, fig. 9.
36. *Quinqueloculina pygmaea* (Reuss) = *Quinqueloculina pygmaea* Reuss, 1850, p. 384, pl. 50, fig. 3 — Boltovskoy, 1978, pl. 6, figs. 32, 33.
37. *Quinqueloculina weaveri* (Rau) = *Quinqueloculina weaveri* Rau, 1948, p. 159, pl. 28, figs. 1–3 — Gupta, 1994, pl. 1, figs. 10, 17.
38. *Robulus gibbus* (d'Orbigny) = *Cristellaria gibba* d'Orbigny, 1839, p. 63, pl. 7, figs. 20, 21 — Gupta, 1994, pl. 2, fig. 3.
39. *Sigmoilopsis schlumbergeri* (Silvestri) = *Sigmoilina schlumbergeri* Silvestri, 1904, p. 267 and 269, figs. 6–9 — Gupta, 1994, pl. 1, fig. 7.
40. *Siphotextularia catenata* (Cushman) = *Textularia catenata* Cushman, 1911, p. 23, figs. 39–40 — Gupta, 1994, pl. 1, fig. 6.
41. *Sphaeroidina bulloides* (d'Orbigny) = *Sphaeroidina bulloides* d'Orbigny, 1826, p. 267, Mod. 65 — Gupta, 1994, pl. 4, fig. 17.
42. *Stilostomella consobrina* (d'Orbigny) = *Siphonodosaria consobrina* d'Orbigny, 1846 — Hayward, 2002, pl. 3, figs. 10, 11.
43. *Stilostomella fistuca* (Schwager) = *Nodosaria fistuca* Schwager, 1866, p. 216, pl. 5, figs. 36–37 — Hayward, 2002, pl. 3, figs. 41–45.
44. *Stilostomella lepidula* (Schwager) = *Nodosaria lepidula* Schwager, 1866, p. 210, pl. 5, fig. 27, 28 — Srinivasan and Sharma, 1980, pl. 7, figs. 1–6.
45. *Uvigerina hispida* (Schwager) = *Euvigerina hispida* Schwager, 1866, p. 249, pl. 7, fig. 95 — Sarkar et al., 2009, pl. 11, fig. 2.
46. *Uvigerina hispido-costata* (Cushman and Todd) = *Uvigerina hispido-costata* Cushman and Todd, 1945, p. 1–73 — Gupta, 1994, pl. 3, figs. 11–13.
47. *Uvigerina peregrina* (Cushman) = *Uvigerina peregrina* Cushman, 1923, p. 166, pl. 42, figs. 7–10 Gupta, 1994, pl. 3, figs. 14–15
48. *Uvigerina proboscidea* (Schwager) = *Uvigerina proboscidea* Schwager, 1866, p. 250, pl. 7, fig. 96 — Gupta, 1994, pl. 3, figs. 16–18.

References

Altenbach, A.V., Pflaumann, U., Schiebel, R., Thies, A., Timm, M., Trauth, M., 1999. Scaling percentages of benthic foraminifera with flux rates of organic carbon. Journal of Foraminiferal Research 29, 173–185.

Alve, E., 1994. Opportunistic features of the foraminifer *Stainforthia fusiformis*_Williamson: evidence from Frierfjord, Norway. Journal of Micropalaeontology 13, 24.

Alve, E., 1999. Colonization of new habitats by benthic foraminifera: a review. Earth Science Reviews 46, 167–185.

Amos, A.F., Gordon, A.L., Schneider, E.D., 1971. Water masses and circulation pattern in the region of the Blake-Bahama Outer Ridge. Deep-Sea Research 18, 145–165.

Balsam, W.L., Damuth, J.E., 2000. Future investigations of shipboard vs. shore-based spectral data: implication for interpreting Leg 164, sediment composition. Proceedings of Ocean Drilling Program Scientific Results 164, 313–324.

Barker, R.W., 1960. Taxonomic notes on the species figured by H. B. Brady in his "Report on the foraminifera dredged by H. M. S. Challenger during the years 1873–1876". SEPM Special Publication 9, 1–238.

Barmawidjaja, D.M., Jorissen, F.J., Puskaric, S., van der Zwaan, G.J., 1992. Microhabitat selection by benthic foraminifera in the northern Adriatic Sea. Journal of Foraminiferal Research 22, 297–317.

Berggren, W.A., Kent, D.V., Swisher III, C.C., Aubry, M.-P., 1995. A revised Cenozoic geochronology and chronostratigraphy. In: Berggren, W.A. (Ed.), Geochronology, Time Scale and Global Stratigraphic Correlation: SEPM Special Publication, Tulsa, USA, vol. 54, pp. 129–212.

Bernhard, J.M., Alve, E., 1996. Survival, ATP pool, and ultrastructural characterization of benthic foraminifera from Drammensfjord (Norway): response to anoxia. Marine Micropaleontology 28, 5–17.

Bernhard, J., Sen Gupta, B.K., Borne, P.F., 1997. Benthic foraminiferal proxy to estimate dysoxic bottom water oxygen concentrations: Santa Barbara Basin, US Pacific continental margin. Journal of Foraminiferal Research 27 (301), 310.

Boltovskoy, E., 1978. Late Cenozoic deep-sea benthic foraminifera of the Ninetyeast Ridge (Indian Ocean). Marine Geology 26, 139–175.

Bower, A.S., Hunt, H.D., 2000. Lagrangian observation of the deep western boundary current in the North Atlantic Ocean, part I: large-scale pathways and spreading rates. Journal of Oceanography 30, 764–783.

Caralp, M.H., 1989. Size and morphology of the benthic foraminifer *Melonis barleeanum*: relationships with marine organic matter. Journal of Foraminiferal Research 19, 235–245.

Corliss, B.H., 1991. Morphology and microhabitat preferences of benthic foraminifera from the northwest Atlantic Ocean. Marine Micropaleontology 17, 195–236.

Corliss, B.H., Silva, K.A., 1993. Rapid growth of deep-sea benthic foraminifera. Geology 21, 991–994.

Cramer, B.S., Toggweiler, J.R., Wright, J.D., Katz, M.E., Miller, K.G., 2009. Ocean overturning since the Late Cretaceous: inferences from a new benthic foraminiferal isotope compilation. Paleoceanography 24, PA4216. doi:10.1029/2008PA001683.

Curry, W.B., Oppo, D.W., 2005. Glacial water mass geometry and the distribution of $\delta^{13}C$ of ΣCO_2 in the western Atlantic Ocean. Paleoceanography 20, PA1017. doi:10.1029/2004PA001021.

De Rijk, S., Troelstra, S.R., Rohling, E.J., 1999. Benthic foraminiferal distribution in the Mediterranean Sea. Journal of Foraminiferal Research 29, 93–103.

de Mello e Sousa, S.H., Passos, R.F., Fukumoto, M., Almeida da Silveira II, C., Figueira, R.C.L., Koutsoukos, E.A.M., de Mahiques, M.M., Rezende, C.E., 2006. Mid-lower bathyal benthic foraminifera of the Campos Basin, Southeastern Brazilian margin: biotopes and controlling ecological factors. Marine Micropaleontology 61, 40–57.

Denne, R.A., Sen Gupta, B.K., 1991. Association of bathyal foraminifera with water masses in the northwestern Gulf of Mexico. Marine Micropaleontology 17, 173–193.

Dowsett, H.J., Chandler, M.A., Robinson, M.M., 2009. Surface temperatures of the Mid-Pliocene North Atlantic Ocean: implications for future climate. Philosophical Transactions of the Royal Society A 367, 69–84.

Evans, H.K., Hall, I.R., 2008. Deepwater circulation on Blake Outer Ridge (western North Atlantic) during the Holocene, Younger Dryas, and Last Glacial Maximum. Geochemistry, Geophysics, Geosystems 9 (Q03023), 19. doi:10.1029/2007GC001771.

Fehn, U., Snyder, G., Egeberg, P.K., 2000. Dating of pore waters with ^{129}I: relevance for the origin of marine gas hydrates. Science 289, 2332–2335.

Fontanier, C., Jorissen, F.J., Chaillou, G., Anschutz, P., Grémare, A., Griveaud, C., 2005. Live foraminiferal faunas from a 2800 m deep lower canyon station from the Bay of Biscay: faunal response to focusing of refractory organic matter. Deep-Sea Research Part-I 52, 1189–1227.

Frank, M., Whiteley, N., Kasten, S., Hein, R., O'Nions, K., 2002. North Atlantic Deep Water export to the Southern Ocean over the past 14 Myr: evidence from Nd and Pb isotopes in ferromanganese crusts. Paleoceanography 17. doi:10.1029/2000 PA000606.

Franz, S.O., Tiedemann, R., 2002. Depositional changes along the Blake-Bahama Outer Ridge deep water transect during marine isotope stages 8 to 10 — links to the Deep Western Boundary Current. Marine Geology 189, 107–122.

Giosan, L., Flood, R.D., Aller, R.C., 2002. Paleoceanographic significance of sediment color on western North Atlantic drifts: I. Origin of color. Marine Geology 189, 25–41.

Gooday, A.J., 2003. Benthic foraminifera (protista) as tools in deep-water paleoceanography: environmental influences on faunal characteristics. Advances in Marine Biology 46, 1–90.

Gupta, A.K., 1993. Biostratigraphic vs. paleoceanographic importance of *Stilostomella lepidula* (Schwager) in the Indian Ocean. Micropaleontology 39, 47–51.

Gupta, A.K., 1994. Taxonomy and bathymetric distribution of Holocene deep-sea benthic foraminifera in the Indian Ocean and the Red Sea. Micropaleontology 40, 351–367.

Gupta, A.K., Thomas, E., 1999. Latest Miocene–Pleistocene productivity and deep-sea ventilation in the northwestern Indian Ocean (DSDP Site 219). Paleoceanography 14, 62–73.

Gupta, A.K., Thomas, E., 2003. Initiation of Northern Hemisphere glaciation and strengthening of the northeast Indian monsoon: Ocean Drilling Program Site 758, eastern equatorial Indian Ocean. Geology 31, 47–50.

Gupta, A.K., Dhingra, H., Melice, J.-C., Anderson, D.M., 2001. Earth's eccentricity cycles and Indian Summer Monsoon variability over the past 2 million years: evidence from deep-sea benthic foraminifer. Geophysical Research Letters 28, 4131–4134.

Gupta, A.K., Sarkar, S., Mukherjee, B., 2006a. Paleoceanographic changes during the past 1.9 Myr at DSDP Site 238, Central Indian Ocean Basin: benthic foraminiferal proxies. Marine Micropaleontology 60, 157–166.

Gupta, A.K., Das, M., Bhaskar, K., 2006b. South Equatorial Current (SEC) driven changes at DSDP Site 237, Central Indian Ocean, during the Plio–Pleistocene: evidence from benthic foraminifera and stable isotopes. Journal of Asian Earth Sciences 28, 276–290.

Gupta, A.K., Sundar Raj, M., Mohan, K., De, S., 2008. A major change in monsoon-driven productivity in the tropical Indian Ocean during ca 1.2–0.9 Myr: foraminiferal faunal and stable isotope data. Palaeogeography, Palaeoclimatology, Palaeoecology 261, 234–245.

Gustafsson, M., Nordberg, K., 2001. Living (stained) benthic foraminiferal response to primary production and hydrography in the deepest part of the Gullmar Fjord, Swedish west coast, with comparisons to Höglund's 1927 material. Journal of Foraminiferal Research 31, 2–11.

Gutjahr, M., Frank, M., Stirling, C.H., Keigwin, L.D., Halliday, A.N., 2008. Tracing the Nd isotope evolution of North Atlantic Deep and Intermediate Waters in the western North Atlantic since the Last Glacial Maximum from Blake Ridge sediments. Earth and Planetary Science Letters 266, 61–77.

Hagen, S., Keigwin, L.D., 2002. Sea-surface temperature variability and deep water reorganisation in the subtropical North Atlantic during Isotope Stage 2–4. Marine Geology 189, 145–162.

Hald, M., Korsun, S., 1997. Distribution of modern benthic foraminifera from fjords of Svalbard, European Arctic. Journal of Foraminiferal Research 27, 101–122.

Haskell, B.J., Johnson, T.C., Showers, W.J., 1991. Fluctuations in deep western North Atlantic circulation on the Blake Outer Ridge during the last deglaciation. Paleoceanography 6, 21–31.

Haug, G.H., Tiedemann, R., 1998. Effect of the formation of the Isthmus of Panama on Atlantic Ocean thermohaline circulation. Nature 393, 673–676.

Haug, G.H., Ganopolski, A., Sigman, D.M., Rosell-Mele, A., Swann, G.E.A., Tiedemann, R., Jaccard, S.L., Bollmann, J., Maslin, M.A., Leng, M.J., Eglinton, G., 2005. North Pacific seasonality and the glaciation of North America 2.7 million years ago. Nature 433, 821–825.

Hayward, B.W., 2002. Late Pliocene to middle Pleistocene extinctions of deep-sea benthic foraminifera ("Stilostomella extinction") in the southwest Pacific. Journal of Foraminiferal Research 32, 274–307.

Hayward, B.W., Neil, H., Carter, R., Grenfell, H.R., Hayward, J.J., 2002. Factors influencing the distribution patterns of Recent deep-sea benthic foraminifera, east of New Zealand, Southwest Pacific Ocean. Marine Micropaleontology 46, 139–176.

Hayward, B.W., Kawagata, S., Grenfell, H.R., Sabaa, A.T., O'Neill, T., 2007. Last global extinction in the deep sea during the mid-Pleistocene climate transition. Paleoceanography 22, PA3103. doi:10.1029/2007PA001424.

Hayward, B.W., Sabaa, A.T., Thomas, E., Kawagata, S., Nomura, R., Schröder-Adams, C., Gupta, A.K., Johnson, K., 2010a. Cenozoic record of elongate, cylindrical, deep-sea benthic foraminifera in the Indian Ocean (ODP Sites 722, 738, 744, 758, and 763). Journal of Foraminiferal Research 40, 113–133.

Hayward, B.W., Johnson, K., Sabaa, A.T., Kawagata, S., Thomas, E., 2010b. Cenozoic record of elongate, cylindrical deep-sea benthic Foraminifera in the North Atlantic and equatorial Pacific Oceans. Marine Micropaleontology 74, 75–95.

Hermelin, J.O.R., Scott, D.B., 1985. Recent benthic foraminifera from the central North Atlantic. Micropaleontology 31, 199–220.

Hermelin, J.O.R., Shimmield, G.B., 1990. The importance of the oxygen minimum zone and sediment geochemistry in the distribution of recent benthic foraminifera in the northwest Indian Ocean. Marine Geology 91, 1–29.

Hill, T.M., Kennett, J.P., Spero, H.J., 2003. Foraminifera as indicators of methane-rich environments: a study of modern methane seeps in Santa Barbara Channel, California. Marine Micropaleontology 49, 123–138.

Ikeda, A., Okada, H., Koizumi, I., 2000. Data report: Late Miocene to Pleistocene diatoms from the Blake Ridge, Site 997. Proceedings of Ocean Drilling Program Scientific Results 164, 365–376.

Jorissen, F.J., 1999. Benthic foraminiferal microhabitats below the sediment–water interface. In: Sen Gupta, B.K. (Ed.), Modern Foraminifera. Kluwer Academic Publishers, Great Britain, pp. 161–179.

Jorissen, F.J., Fontanier, C., Thomas, E., 2007. Paleoceanographical proxies based on deep-sea benthic foraminiferal assemblage characteristics. In: Hillaire-Marcel, C., de Vernal, A. (Eds.), Proxies in Late Cenozoic Paleoceanography: Pt. 2: Biological Tracers and Biomarkers. Elsevier, pp. 263–326.

Kaiho, K., 1998. Phylogeny of deep-sea calcareous trochospiral benthic Foraminifera; evolution and diversification. Micropaleontology 44, 291–311.

Kawagata, S., Hayward, B.W., Grenfell, H.R., Sabba, A.T., 2005. Mid-Pleistocene extinction of deep-sea foraminifera in the North Atlantic Gateway (ODP Sites 980 and 982). Palaeogeography, Palaeoclimatology, Palaeoecology 221, 267–291.

Kroopnick, P.M., 1985. The distribution of ^{13}C of ΣCO_2 in the world ocean. Deep-Sea Research 32, 57–84.

Liu, C., Browning, J.V., Miller, K.G., Olsson, R.K., 1997. Paleocene benthic foraminiferal biofacies and sequence stratigraphy, Island Beach borehole, New Jersey. Proceedings of Ocean Drilling Program Scientific Results 150X, 267–275.

Loubere, P., Fariduddin, F., 1999. Quantitative estimates of global patterns of surface ocean biological productivity and its seasonal variation on time scales from centuries to millennia. Global Biogeochemical Cycles 13, 115–133.

Luo, S., Ku, T.L., Wang, I., Southin, J.R., Lund, S.P., Schwartz, M., 2001. ^{26}Al, ^{10}Be and U–Th isotopes in the Blake Outer Ridge sediments: implications for past changes in boundary scavenging. Earth and Planetary Science Letters 185, 135–147.

Lutze, G.F., 1986. Uvigerina species of the eastern North Atlantic. In: van der Zwaan, G.J., Jorissen, F.J., Verhallen, P.J.J.M., von Daniels, C.H. (Eds.), Atlantic-European Oligocene to Recent Uvigerina, vol. 35. Utrecht Micropaleontological Bulletin, The Netherlands, pp. 47–66.

Lynch-Stieglitz, J., Adkins, J.F., Curry, W.B., Dokken, T., Hall, I.R., Herguera, J.C., Hirschi, J.J.-M., Ivanova, E.V., Kissel, C., Marchal, O., Marchitto, T.M., McCave, I.N., McManus, J.F., Mulitza, S., Ninnemann, U., Peeters, F., Yu, E.-F., Zahn, R., 2007. Atlantic meridional overturning circulation during the last glacial maximum. Science 316, 66–69.

Mackensen, A., Sejrup, H.P., Janse, E., 1985. Living benthic foraminifera off Norway. Marine Micropaleontology 9, 275–306.

Mackensen, A., Schmiedl, G., Harloff, J., Giese, M., 1995. Deep-sea foraminifera in the South Atlantic Ocean: ecology and assemblage generation. Micropaleontology 41, 342–358.

Marchitto, T.M., Curry, W.B., Oppo, D.W., 1998. Millennial-scale changes in North Atlantic Circulation since the last glaciation. Nature 393, 557–561.

Marszalek, D.S., Wright, R.C., Hay, W.W., 1969. Function of the test in foraminifera. Transactions—Gulf coast association of Geological Societies XIX, pp. 341–352.

Maslin, M.A., Li, X.S., Loutre, M.-F., Berger, A., 1998. The contribution of orbital forcing to the progressive intensification of Northern Hemisphere Glaciation. Quaternary Science Reviews 17, 411–426.

McClymont, E.L., Rosell-Melé, A., 2005. Links between the onset of modern Walker Circulation and the mid-Pleistocene climate transition. Geology 33, 389–392.

McDougall, K., 1996. Benthic foraminiferal response to the emergence of the isthmus of Panama and coincident paleoceanographic changes. Marine Micropaleontology 28, 133–169.

Millo, C., Sarnthein, M., Erlenkeuser, H., Grootes, P.M., Andersen, N., 2005. Methane-induced early diagenesis of foraminiferal tests in the southwestern Greenland Sea. Marine Micropaleontology 58, 1–12.

Mudelsee, M., Raymo, M.E., 2005. Slow dynamics of the Northern Hemisphere glaciation. Paleoceanography 20, PA4022. doi:10.1029/2005PA001153.

Mullineaux, L.S., Lohmann, G.P., 1981. Late Quaternary stagnations and recirculation of the eastern Mediterranean: changes in the deep water recorded by fossil benthic foraminifera. Journal of Foraminiferal Research 11, 20–39.

Murgese, D.S., Deckker, P.D., 2005. The distribution of deep-sea benthic foraminifera in core tops from the eastern Indian Ocean. Marine Micropaleontology 56, 25–49.

Murray, J.W., 2006. Ecology and Application of Benthic Foraminifera. Cambridge University Press, Cambridge, pp. 220–221.

Nees, S., Struck, U., 1999. Benthic foraminiferal response to major paleoceanographic changes. In: Abrantes, F., Mix, A. (Eds.), Reconstructing Ocean History: A Window into the Future. Kluwer Academic Plenum Publishers, New York, pp. 195–216.

Okada, H., 2000. Neogene and Quaternary calcareous nannofossils from the Blake Ridge, Sites 994, 995, and 997. Proceedings of Ocean Drilling Program Scientific Results 164, 331–341.

Pagani, M., Liu, Z., LaRiviere, J., Ravelo, A.C., 2010. High Earth-system climate sensitivity determined from Pliocene carbon dioxide concentrations. Nature Geoscience 3, 27–30. doi:10.1038/ngeo724.

Paull, C.K., Matsumoto, R., Wallace, P.J., Shipboard Scientific Party, 1996. Gas hydrate sampling on the Blake Ridge and Carolina Rise sites 991–997. Proceedings of Ocean Drilling Program Initial Report 164, 99–318.

Pierre, C., Rouchy, J.M., Gaudichet, A., 2000. Diagenesis in the gas hydrate sediments of the Blake Ridge: mineralogy and stable isotope compositions of the carbonate and sulfide minerals. Proceedings of Ocean Drilling Program Scientific Results 164, 229–236.

Pollard, D., deConto, R.M., 2009. Modelling West Antarctic ice sheet growth and collapse through the past five million years. Nature 458, 329–333.

Poore, H.R., Samworth, R., White, N.J., Jones, S.M., McCave, I.N., 2006. Neogene overflow of Northern Component water at the Greenland–Scotland Ridge. Geochemistry, Geophysics, Geosystems 7 (6), Q06010. doi:10.1029/2005/GC001085.

Rasmussen, T.L., Thomsen, E., Troelstra, S.R., Kuijpers, A., Prins, M.A., 2002. Millennial-scale glacial variability versus Holocene stability: changes in planktic and benthic foraminifera faunas and ocean circulation in the North Atlantic during the last 60000 years. Marine Micropaleontology 47, 143–176.

Rathburn, A.E., Corliss, B.H., 1994. The ecology of living (stained) benthic foraminifera from the Sulu Sea. Paleoceanography 9, 87–150.

Rathburn, A.E., Levin, L.A., Held, Z., Lohmann, K.C., 2000. Benthic foraminifera associated with cold methane seeps on the northern California margin: ecology and stable isotopic composition. Marine Micropaleontology 38, 247–266.

Ravelo, A.C., Hillaire-Marcel, C., 2007. The use of oxygen and carbon isotopes of foraminifera in paleoceanography. In: Hillaire-Marcel, C., De Verna, A. (Eds.), Proxies in Late Cenozoic Paleoceanography. : Developments in Marine Geology, 1. Elsevier, The Netherlands, pp. 735–764.

Raymo, M.E., Rind, D., Ruddiman, W.F., 1990. Climatic effects of reduced Arctic sea ice limits in the GISS II general circulation model. Paleoceanography 5, 367–382.

Raymo, M.E., Ganley, K., Carter, S., Oppo, D.W., McManus, J., 1998. Millennial-scale climate instability during the early Pleistocene epoch. Nature 392, 699–702.

Reynolds, B.C., Frank, M., O'Nions, R.K., 1999. Nd- and Pb-isotope time series from Atlantic ferromanganese crusts: implications for changes in provenance and paleocirculation over the last 8 Myr. Earth and Planetary Science Letters 173, 381–396.

Robinson, C.A., Bernhard, J.M., Levin, L.A., Mendoza, G.F., Blanks, J.K., 2004. Surficial hydrocarbon seep infauna from the Blake Ridge (Atlantic Ocean, 2150 m) and the Gulf of Mexico (690–2240 m). Marine Ecology 25 (4), 313–336.

Roth, S., Reijmer, J.J.G., 2004. Holocene Atlantic climate variations deduced from carbonate peri-platform sediments (leeward margin, Great Bahama Bank). Paleoceanography 19 (1), PA1003. doi:10.1029/2003PA000885.

Sarkar, S., De, S., Gupta, A.K., 2009. Late Quaternary benthic foraminifera from Ocean Drilling Program Hole 716A, Maldives Ridge, southeastern Arabian Sea. Micropaleontolology 55, 23–48.

Schmiedl, G., Mackensen, A., 1997. Late Quaternary paleoproductivity and deep water circulation in the eastern South Atlantic Ocean: evidence from benthic foraminifera. Palaeogeography, Palaeoclimatology, Palaeoecology 130, 43–80.

Schmiedl, G., Mackensen, A., Müller, P.J., 1997. Recent benthic foraminifera from the eastern South Atlantic Ocean: dependence on food supply and water masses. Marine Micropaleontology 32, 249–287.

Schmiedl, G., de Bovée, F., Buscail, R., Charrière, B., Hemleben, Ch., Medernach, L., Picon, P., 2000. Trophic control of benthic foraminiferal abundance and microhabitat in the bathyal Gulf of Lions, western Mediterranean Sea. Marine Micropaleontology 40, 167–188.

Schnitker, D., 1986. North-east Atlantic Neogene benthic foraminiferal faunas: traces of deep-water paleoceanography. In: Summerhayes, C.P., Shackleton, N.J. (Eds.), North Atlantic Paleoceanography, vol. 21. Geological Society Special Publication, London, pp. 191–203.

Seki, O., Foster, G.L., Schmidt, D.N., Mackensen, A., Kawamura, K., Pancost, R.D., 2010. Alkenone and boron-based Pliocene pCO_2 records. Earth and Planetary Science Letters 292, 201–211.
Sen Gupta, B.K., Machain-Castillo, M.L., 1993. Benthic foraminifera in oxygen-poor habitats. Marine Micropaleontology 20, 183–201.
Shackleton, N.J., Hall, M.A., Boersma, A., 1984. Oxygen and carbon isotope data from Leg 74 foraminifers. Deep Sea Drilling Project Initial Report 74, 599–612.
Shipboard Scientific Party, 1998. Introduction. Proceedings of Ocean Drilling Program Initial Reports 172, 7–12.
Singh, R.K., Gupta, A.K., 2004. Late Oligocene–Miocene paleoceanographic evolution of the southeastern Indian Ocean: evidence from deep-sea benthic foraminifera (ODP Site 757). Marine Micropaleontology 51, 153–170.
Smart, C.W., Thomas, E., Ramsay, A.T.S., 2007. Middle–late Miocene benthic foraminifera in a western equatorial Indian Ocean depth transect: paleoceanographic implications. Palaeogeography, Palaeoclimatology, Palaeoecology 247, 402–420.
Srinivasan, M.S., Sharma, V., 1980. Schwagers Car Nicobar Foraminifera in the Reports of the 'Novara' Expedition — Revision. Today and Tomorrow' Printers and Publishers, New Delhi, pp. 1–83.
Stahr, F.R., Sanford, T.B., 1999. Transport and bottom boundary layer observations of the North Atlantic Deep Western Boundary Current at the Blake Outer Ridge. Deep-Sea Research II 46, 205–243.
Thomas, E., 2007. Cenozoic mass extinctions in the deep sea: what perturbs the largest habitat on earth? In: Monechi, S., Coccioni, R., Rampino, M.R. (Eds.), Mass Extinctions and Other Large Ecosystem Perturbations: Extraterrestrial and Terrestrial Causes: Geological Society of America Special Paper, vol. 424, pp. 1–23.
Thunell, R.C., Poli, M.S., Rio, D., 2002. Changes in deep and intermediate water properties in the western North Atlantic during marine isotope stages 11–12: evidence from ODP Leg 172. Marine Geology 189, 63–77.
Van Dover, C.L., Aharon, P., Bernhard, J.M., Caylor, E., Doerries, M., Flickinger, W., Gilhooly, W., Goffredi, S.K., Knick, K.E., Macko, S.A., Rapoport, S., Raulfs, E.C., Ruppel, C., Salerno, J.L., Seitz, R.D., Sen Gupta, B.K., Shank, T., Turnipseed, M., Vrijenhoek, R., 2003. Blake Ridge methane seeps: characterization of a soft-sediment, chemosynthetically based ecosystem. Deep-Sea Research I 50, 281–300.
Wara, M.W., Ravelo, A.C., Delaney, M.L., 2005. Permanent El Niño-like conditions during the Pliocene warm period. Science 309, 758–761.
Weatherly, G.L., Kelley Jr., E.A., 1985. Two views of the cold filament. Journal of Physical Oceanography 15, 68–81.
Wefer, G., Heinze, P.-M., Berger, W.H., 1994. Clues to ancient methane release. Nature 369, 282.
Wright, J.D., Miller, K.G., 1996. Control of North Atlantic deep water circulation by the Greenland–Scotland Ridge. Paleoceanography 11, 157–170. doi:10.1029/95PA03696.
Zachos, J., Pagani, M., Sloan, L., Thomas, E., Billups, K., 2001. Trends, rhythms, and aberrations in global climate 65 Ma to present. Science 292, 686–693.